The Roles of Aminocarbyne Intermediates and Intramolecular Electron Transfer in the Formation of Carbon–Carbon Bonds by the Coupling of Isocyanides

Jianxin Wu,[1] Phillip E. Fanwick,[2] and Clifford P. Kubiak*,[3]

Contribution from the Department of Chemistry, Purdue University, West Lafayette, Indiana 47907. *Received February 28, 1989*

Abstract: The binuclear iridium complex $Ir_2(CNR)_4(dmpm)_2$, **1**, (R = 2,6-$Me_2C_6H_3$, dmpm = $Me_2PCH_2PMe_2$) was prepared by reduction of $[Ir_2(CNR)_5(dmpm)_2][PF_6]_2$ with Na amalgam in benzene. The structure of **1**, determined by X-ray diffraction, consists of two iridium atoms bridged by two cis,cis dmpm ligands and two μ-2,6-xylyl isocyanide ligands. The Ir–Ir bond length is 2.5998 (7) Å. The nonbonded distance between the carbon atoms of the μ-isocyanide ligands is 2.37 (2) Å. The potential coupling of the two μ-isocyanide ligands of **1**, promoted by Lewis acids, was investigated. Addition of 2 equiv of BH_3·THF to **1** affords $Ir_2(\mu\text{-}CN(BH_3)R)_2(CNR)_2(dmpm)_2$, **2**, which contains two μ-$CN(BH_3)R$ aminocarbyne groups which are not coupled. Addition of Al_2Et_6 to **1** in toluene gives $Ir_2(C_2(NR)_2AlEt_2)(CNR)_2(dmpm)_2$, **3**, which contains a new carbon–carbon bond, d(C–C) = 1.48 (1) Å, between two coupled isocyanides. The $AlEt_2$ fragment bridges two isocyanide N atoms to form an essentially planar five-membered C_2N_2Al ring. The C_2N_2Al ring is coplanar with the two iridium atoms. Complex **3** is paramagnetic and exhibits an isotropic EPR powder spectrum, g = 2.005 at −150 °C. Complex **3** is reversibly oxidized electrochemically to form the diamagnetic species $[Ir_2\{C_2(NR)_2AlEt_2\}(CNR)_2(dmpm)_2][PF_6]$, **4**. $E_{1/2}$(**4**/**3**) = −0.22 V vs SCE. The mechanism of isocyanide coupling leading to **3** involves electronic reconfiguration of the d^9–d^9 Ir^0_2 core of **1** to the d^8–d^8 Ir^I_2 "A-frame" species **4**. Paramagnetic **3** is formed by single-electron transfer to **4** by $AlEt_4^-$, formed in situ during isocyanide coupling. Crystal data for **1**: space group $P2_1$; a = 10.615 (2), b = 16.883 (3), c = 15.044 (3) Å; β = 94.23 (1)°; V = 2689 (2) Å^3; Z = 2; R = 0.033, R_w = 0.044 for 528 variables and 3229 unique data with $I > 3\sigma(I)$, Mo Kα radiation. Crystal data for **2**: space group $P2_12_12$; a = 15.905 (2), b = 16.286 (2), c = 10.528 (3) Å; Z = 2; V = 2727 (1) Å^3; R = 0.048, R_w = 0.062 for 282 variables and 2263 unique data with $I > 3\sigma(I)$, Mo Kα radiation. Crystal data for **3**: space group $P2_1/c$; a = 11.44 (1), b = 19.072 (1), c = 25.602 (3) Å; β = 102.91°; V = 5446 (2) Å^3; Z = 4; R = 0.035, R_w = 0.040 for 550 variables and 5330 unique data with $I > 3\sigma(I)$, Mo Kα radiation.

Among the more important reactions in organometallic chemistry are those resulting in formation of a new carbon–carbon bond. There has been a particularly keen interest in coupling pairs of coordinated carbonyl[4-6] or isocyanide[7,8] ligands of mononuclear[5,7] and binuclear[4,6] transition-metal complexes. We describe herein our studies of carbon–carbon bond forming reactions between a pair of μ-isocyanide ligands of a binuclear iridium complex, $Ir_2(\mu\text{-}CNR)_2(CNR)_2(dmpm)_2$ (R = 2,6-$Me_2C_6H_3$, dmpm = bis(dimethylphosphino)methane) (**1**). These coupling reactions

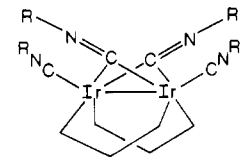

1

R = 2,6-$Me_2C_6H_3$, ⌒ = $Me_2PCH_2PMe_2$

are unusual in several respects.[9,10] They represent rare examples of coupling reactions mediated by a late-transition-metal complex, a d^9–d^9 Ir(0) system. The coupling reactions do not require two external reducing equivalents. Instead, the two electrons essential for the creation of a new carbon–carbon bond are derived from electronic reconfiguration of the complex to a formally d^8–d^8 Ir(I) system, induced by a Lewis acid. The work described is part of an ongoing effort to elucidate the chemical and photochemical reactivity of molecules spanning two metal centers. The new diiridium complex **1** possesses structure II and is related to a series of d^{10}–d^{10}, $Ni_2(\mu\text{-L})L_2'(PPh_2CH_2PPh_2)_2$ "cradle"-type complexes of structure I.

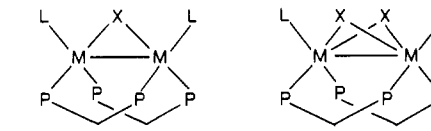

I d^{10}–d^{10}, μ-X II d^9–d^9, $(\mu\text{-X})_2$

The chemistry,[11a] electrochemistry,[11b] and photochemistry[11c,d] of the d^{10}–d^{10} (μ-X), structure type I systems were recently reported. In preparing complex **1**, our idea was to exploit the structural and electronic features of the cis-$(\mu\text{-X})_2$ framework to study carbon–carbon bond formation between μ-X ligands.

We report the preparation of the binuclear Ir(0) complex, $Ir_2(\mu\text{-}CNR)_2(CNR)_2(dmpm)_2$, **1**, (R = 2,6-$Me_2C_6H_3$), its solid-state structure as determined by X-ray diffraction, and the reactivity of **1** toward C···C coupling of the μ-isocyanide ligands. The reaction of **1** with BH_3·THF to afford a bis(μ-aminocarbyne) complex $Ir_2(\mu\text{-}CN(BH_3)R)_2(CNR)_2(dmpm)_2$ (R = 2,6-MeC_6H_3) (**2**) and the X-ray structure of **2**, which indicates a distinctly

(1) Present address: Department of Chemistry, University of California, Berkeley, California 94720.

(2) Address correspondence pertaining to crystallographic studies to this author.

(3) Research Fellow of the Alfred P. Sloan Foundation, 1987–1991.

(4) (a) Berry, D. H.; Bercaw, J. E.; Jircitano, A. J.; Mertes, K. *J. Am. Chem. Soc.* **1982**, *104*, 4712. (b) Wolczanski, P. T.; Bercaw, J. E. *Acc. Chem. Res.* **1980**, *13*, 121. (c) Manriquez, J. M.; McAlister, D. R.; Sanner, R. D.; Bercaw, J. E. *J. Am. Chem. Soc.* **1978**, *100*, 2716.

(5) Bianconi, P. A.; Williams, I. D.; Engeler, M. P.; Lippard, S. J. *J. Am. Chem. Soc.* **1986**, *108*, 311.

(6) (a) Nasta, M. A.; MacDiarmid, A. G.; Saalfeld, F. E. *J. Am. Chem. Soc.* **1972**, *94*, 2449. (b) Bennett, M. J.; Graham, W. A. G.; Smith, R. A.; Steward, R. P., Jr. *J. Am. Chem. Soc.* **1973**, *95*, 1684.

(7) (a) Lam, C. T.; Corfield, P. W. R.; Lippard, S. J. *J. Am. Chem. Soc.* **1977**, *99*, 617. (b) Corfield, P. W. R.; Baltusis, L. M.; Lippard, S. J. *Inorg. Chem.* **1981**, *20*, 922. (c) Dewan, J. C.; Giandomenico, C. M.; Lippard, S. J. *Ibid.* 4069. (d) Dewan, J. C.; Lippard, S. J. *Ibid.* **1982**, *21*, 1682. (e) Giandomenico, C. M.; Lam, C. T.; Lippard, S. J. *J. Am. Chem. Soc.* **1982**, *104*, 1263.

(8) Wu, J.; Fanwick, P. E.; Kubiak, C. P. *J. Am. Chem. Soc.* **1988**, *110*, 1319.

(9) Hoffmann, R.; Wilker, C. N.; Lippard, S. J.; Templeton, J. S.; Brower, D. C. *J. Am. Chem. Soc.* **1983**, *105*, 146.

(10) Bergman, R. G. *Acc. Chem. Res.* **1980**, *13*, 113.

(11) (a) DeLaet, D. L.; Fanwick, P. E.; Kubiak, C. P. *Organometallics* **1986**, *5*, 1807. (b) DeLaet, D. L.; Del Rosario, R.; Fanwick, P. E.; Kubiak, C. P. *J. Am. Chem. Soc.* **1987**, *109*, 754. (c) DeLaet, D. L.; Fanwick, P. E.; Kubiak, C. P. *J. Chem. Soc., Chem. Commun.* **1987**, 1412. (d) Lemke, F. R.; DeLaet, D. L.; Gao, J.; Kubiak, C. P. *J. Am. Chem. Soc.* **1988**, *110*, 6904.

0002-7863/89/1511-7812$01.50/0

uncoupled pair of μ-CN(BH_3)R ligands, are also described. The chemistry of **1** with Al_2Et_6 and the structure of the coupled isocyanide complex $Ir_2(\eta^2$-$(CNR)_2AlEt_2)(CNR)_2(dmpm)_2$ (R = 2,6-$Me_2C_6H_3$) (**3**) are reported. Isocyanide coupling reactions of **1** with other reagents and the stereoelectronic factors that appear to control isocyanide coupling in these systems are discussed.

Experimental Section

Materials. All solvents were reagent grade and were distilled from appropriate drying agents. 2,6-Dimethylphenyl isocyanide was purchased from Fluka Chemical Corp. Iridium trichloride was obtained on loan from Johnson-Matthey, Inc. Bis(dimethylphosphino)methane[12] and $[Ir(COD)Cl]_2$[13] were prepared by literature procedures. Triethylaluminum was purchased from Alfa Products. The preparation of $[Ir_2(CNR)_5(dmpm)_2][PF_6]_2$ (R = 2,6-$Me_2C_6H_3$) was described previously.[14] All reactions were performed under an atmosphere of dry nitrogen.

Physical Measurements. Elemental analyses were performed by the Microanalytical Laboratory of the Department of Chemistry, Purdue University, and by Galbraith Laboratories of Knoxville, TN. ^1H NMR spectra were recorded on a Varian XL-200 spectrometer. ^{31}P NMR spectra were recorded on a Varian XL-200 spectrometer operating at 81 MHz with broad-band proton decoupling. The variable-temperature ^{31}P NMR studies were performed with a Nicolet-470 spectrometer. The ^{31}P chemical shifts are reported relative to external 85% H_3PO_4. Infrared spectra were recorded on a Perkin-Elmer 1710 Fourier transform infrared spectrophotometer. UV–vis spectra were measured on an IBM 9420 UV–visible spectrophotometer. X-band EPR spectra were recorded on a Varian E-109 spectrometer. Electrochemical measurements were performed with Princeton Applied Research, Model 173 Potentiostat/Galvanostat and Model 175 Universal Programmer in conjunction with a Hewlett-Packard 7045B X-Y recorder.

Preparation of $Ir_2(\mu$-$CNR)_2(CNR)_2(dmpm)_2$ (R = 2,6-Me_2-C_6H_3) (1). Method A. A slurry of $[Ir_2(CNR)_5(dmpm)_2][PF_6]_2$ (R = 2,6-Me_2-C_6H_3)[14] (2.00 g) in 200 mL of benzene and excess sodium amalgam was stirred for 3 days. The resulting dark orange solution was decanted and filtered, and benzene was evaporated under vacuum. Free isocyanide was removed by washing the residue three times with 6-mL portions of benzene to give **1** as a bright yellow solid. Recrystallization of **1** from benzene/hexanes afforded crystals as a benzene solvate. The benzene molecule of solvation was only partly removable under high vacuum. This affected the quality of microanalyses. Isolated yield: 1.24 g (85%).

Method B. To 150 mL of benzene was added $[Ir(COD)Cl]_2$ (1.00 g, 1.49 mmol), 2,6-xylyl isocyanide (0.78 g, 5.95 mmol), and bis(dimethylphosphino)methane (0.46 mL, 2.98 mmol). The mixture was stirred with excess sodium amalgam for 36 h. The solution was decanted from the bulk of the amalgam and filtered. Benzene was removed under vacuum. The residue was washed three times with 5-mL portions of fresh benzene and dried in vacuo. Complex **1** was obtained as a bright yellow solid (0.82 g, 47%). Anal. Calcd for $Ir_2P_4N_4C_{48}H_{66}$ (**1**·$^1/_3C_6H_6$): C, 47.75; H, 5.51; N, 4.64. Found: C, 47.55; H, 5.72; N, 4.43. ^1H NMR ($CD_3C_6D_5$): δ 6.9 (m, 12 H), 2.51 (s, 12 H), 2.37 (s, 12 H), 1.70 (s, 12 H), 1.08 (s, 12 H), 0.89 (q, 4 H). ^{31}P NMR (C_6D_6): δ −34.7 (s, br). IR (KBr): ν(CN) 2038 (s), 1996 (s, br), 1626 (sh), 1600 (s); ν(PC) 945 (s), 926 (s) cm^{-1}. IR (toluene): ν(CN) 2040 (s), 2008 (s), 1631 (w), 1605 (m) cm^{-1}. UV–vis (benzene): 300 nm (ϵ 27 000), 384 (ϵ 4240).

Preparation of $Ir_2(\mu$-$CNR(BH_3))_2(CNR)_2(dmpm)_2$, 2. Complex **1** (0.10 g) was dissolved in 30 mL of benzene solution, and excess BH_3·THF was added while stirring. A white precipitate formed immediately, which was filtered, washed twice with diethyl ether, and dried under vacuum. Recrystallization from methylene chloride/diethyl ether afforded crystals of **2** with one methylene chloride of solvation. The CH_2Cl_2 molecule of solvation was confirmed by ^1H NMR in CD_3CN. Isolated yield: 0.10 g (92%). Anal. Calcd for $Ir_2P_4Cl_2B_2N_4C_{47}H_{72}$ (**2**·CH_2Cl_2): C, 43.64; H, 5.61; N, 4.33. Found: C, 43.93; H, 6.01; N, 4.48. ^1H NMR (CD_2Cl_2): δ 7.03 (m, 6 H), 6.78 (d, 2 H), 6.68 (t, 2 H), 6.49 (d, 2 H), 2.45 (s, 12 H), 2.31 (s, 12 H), 2.23 (d, 6 H), 1.80 (m, 4 H), 1.52 (dd, 12 H), 1.43 (m, 6 H) (the BH_3 protons were not located in the ^1H NMR). ^{31}P NMR (CD_2Cl_2): δ −37.1 (AA′BB′). IR (KBr): ν(CN) 2057 (s), 2009 (m), 1520 (sh), 1500 (m); ν(PC) 949 (m), 933 (m) cm^{-1}. IR (CH_2Cl_2): ν(CN) 2063 (s), 2009 (m), 1520 (m), 1502 (m) cm^{-1}.

Preparation of $Ir_2(\eta^2$-$(CNR)_2AlEt_2)(CNR)_2(dmpm)_2$, 3. To a toluene solution containing 137 mg of **1** (0.11 mmol) was added 34 μL of neat Al_2Et_6 (0.24 mmol, 95% purity, 1 equiv). The mixture was stirred for 2 days in a closed flask under N_2. Approximately 0.08 mmol of C_2H_4 and 0.02 mmol of C_2H_6 were detected by gas chromatography. The dark red-purple solution was decanted and hexanes were slowly diffused into the solution. Dark red-purple crystals were collected, washed with hexanes, and dried. Isolated yield: 30 mg (22%). Anal. Calcd for $Ir_2AlP_4N_4C_{50}H_{74}$ (**3**): C, 47.44; H, 5.89; N, 4.42. Found: C, 46.50; H, 6.06; N, 4.08. IR (KBr): ν(CN) 2047 (s), 1996 (s); ν(PC) 935 (m, br) cm^{-1}.[15] UV–vis (toluene): 574 nm (ϵ 6400), 876 (ϵ 400).

Reaction of 1 with BF_3·OEt_2. To 4 mL of THF containing 0.01 g of **1** was added 2 μL of BF_3·OEt_2 (2 equiv). A pale yellow solid formed immediately, which was filtered, washed with benzene, and dried. IR (KBr): ν(CN) 2162 (s), 2087 (s), 1507 (w); ν(PC) 943 (s) cm^{-1}. The IR spectra of the THF and CH_2Cl_2 solutions are significantly different from the solid-state IR spectrum, indicating the complex decomposes in these solvents. IR (THF): 2109 (sh), 2092 (s), 1510 (w) cm^{-1}. IR (CH_2Cl_2): 2133 (sh), 2116 (s) cm^{-1}. $^{31}P\{^1H\}$ NMR (acetone): δ −48.6 (s). Low-temperature reactions were conducted in attempts to obtain single crystals by slow reaction. A toluene solution (5 mL) containing 0.04 g of **1** was frozen at liquid N_2 temperature and 10 μL of BF_3·OEt_2 (2.5 equiv) was added. The solution was warmed slowly to −78 °C and kept at that temperature for several days. Noncrystalline solids were formed repeatedly. IR (KBr): ν(CN) 2162 (s), 2087 (s), 1507 (m); ν(PC) 943 (s); ν(BF) 1087 (s), 1060 (vs), 1037 (s) cm^{-1}.

Reaction of 1 with Maleic Anhydride. To a 25-mL benzene solution containing 0.1 g of **1** was added 0.02 g (2 equiv) of maleic anhydride dissolved in 2 mL of benzene. A red solid formed immediately. After stirring for 1 h, the solid was collected by filtration, washed twice with benzene, and dried. Isolated yield: 0.08 g. The solid is soluble but not stable in CH_3CN or CH_2Cl_2. The solid is insoluble in THF, benzene, and toluene. IR (KBr): ν(CN) 2110 (sh), 2089 (s), 1615 (m), 1585 (m); ν(CO): 1781 (m), 1730 (m); ν(PC) 941 (s) cm^{-1}. IR (CH_2Cl_2): ν(CN) 2115 (sh), 2092 (s), 2001 (w), 1638 (m), 1586 (m); ν(CO) 1858 (w), 1781 (m), 1732 (m) cm^{-1}. $^{31}P\{^1H\}$ NMR (CH_2Cl_2): δ −43.9 (s); (CH_3CN) −43.3 (s).

Reaction of 1 with 1,4-Benzoquinone. To 4 mL of THF containing 0.03 g of **1** was added 0.5 mL of THF containing 0.004 g (1.4 equiv) of 1,4-benzoquinone. The solution turned dark orange and solids precipitated out. After stirring for 2 h, the solids were filtered, washed with THF, and dried. IR (KBr): ν(CN) 2077 (s), 1620 (w), 1583 (w); ν(PC) 941 (s) cm^{-1}. The solid is insoluble in most solvents and a $^{31}P\{^1H\}$ NMR (CH_2Cl_2) could not be recorded.

Oxidation of 3 by $[Cp_2Fe][PF_6]$. To 3 mL of THF containing 6 mg of **3** was added 1.5 mg (1 equiv) of $[Cp_2Fe][PF_6]$ in 1.5 mL of THF. The red-purple color of the solution changed to yellow upon completion of the addition. The product was precipitated by addition of pentane and collected by filtration, washed by pentane, and dried. IR (KBr): ν(CN) 2123 (s); ν(PC) 943 (s) cm^{-1}. $^{31}P\{^1H\}$ (THF): δ −43.3 (s).

Electrochemistry of 3. Cyclic voltammetric studies of **3** were carried out under N_2 in THF containing 0.1 M tetra-*n*-butylammonium tetrafluoroborate (TBAF) as supporting electrolyte. A three-electrode cell configuration was used, with a platinum disk and a platinum wire as working and auxiliary electrodes, respectively. Saturated calomel (SCE) was used as the reference electrode. A reversible oxidation of **3** was observed at −0.22 V vs SCE, with a peak-to-peak separation of 90 mV.

An exhaustive electrolysis of **3** was conducted at E = +0.30 V vs SCE in a three-compartment electrochemical cell. In the anodic compartment was a red-purple THF solution of **3** (4.3 mg). In the cathodic compartment was a blue solution of $[Cp_2Fe][PF_6]$ in THF. The center compartment was connected to the anodic and cathodic compartments via glass frits. TBAF (0.1 M) was used as supporting electrolyte in all three compartments. During electrolysis there was no diffusion of **3** or $[Cp_2Fe][PF_6]$ into the center compartment and the solution in the center compartment remained colorless throughout the electrolysis period. After 3.4 μmol of electrons, corresponding to 1 equiv of **3**, had been passed, the anodic solution turned yellow. The $^{31}P\{^1H\}$ NMR spectrum of the electrolyzed solution exhibits a single peak at δ −43.5 ppm.

Crystal Data Collection and Reduction. $Ir_2(CNR)_4(dmpm)_2$ (R = 2,6-$Me_2C_6H_3$) (1). Single crystals of **1** were obtained by slow diffusion of hexanes into a benzene solution containing complex **1**. The crystal used for data collection was mounted in a capillary tube and sealed with epoxy cement. Three standard reflections were monitored after every 100 reflections, an no decay was noticed over data collection. Crystal data and collection parameters for complex **1** are summarized in Table I. No

(12) Kubiak, C. P.; Kullberg, M. L.; Lemke, F. R.; RaghuVeer, K. S.; King, C.; Roundhill, D. M., submitted for publication in *Inorg. Synth.*

(13) Herde, J. L.; Lambert, J. C.; Senott, C. V. *Inorg. Synth.* **1974**, *15*, 18.

(14) Wu, J.; Reinking, M. K.; Fanwick, P. E.; Kubiak, C. P. *Inorg. Chem.* **1987**, *26*, 247.

(15) The bridging ν(CN) bands in **3** are mixed with bands of 2,6-xylyl groups and dmpm ligands below 1450 cm^{-1}. No bands can be attributed to bridging ν(CN) in the 1700–1450-cm^{-1} region.

Table I. Summary of Crystal Data and Collection Parameters for Complexes 1–3

	1	2	3
formula	$Ir_2P_4N_4C_{52}H_{70}$	$Ir_2P_4ON_4B_2C_{50}H_{78}$	$Ir_2P_4AlN_4C_{50}H_{74}$
fw	1259.5	1281.2	1266.45
space gp	$P2_1$	$P2_12_12$	$P2_1/c$
a, Å	10.615 (2)	15.905 (2)	11.444 (1)
b, Å	16.883 (3)	16.286 (2)	19.072 (1)
c, Å	15.044 (3)	10.528 (3)	25.602 (3)
β, deg	94.23 (1)		102.91 (1)
V, Å^3	2689 (2)	2727 (1)	5446 (2)
Z	2	2	4
d_{calc}, g cm^{-3}	1.555	1.560	1.544
crystal dimens, mm	0.63 × 0.56 × 0.46	0.31 × 0.12 × 0.09	0.38 × 0.24 × 0.20
temp, °C	24.0	22.0	22.0
radiation (wavelength)	Mo Kα (0.71073 Å)	Mo Kα (0.71073 Å)	Mo Kα (0.71073 Å)
monochromator	graphite	graphite	graphite
linear abs coeff, cm^{-1}	50.78	50.08	50.29
abs corr applied	empirical[a]	empirical[a]	empirical[a]
diffractometer	Enraf-Nonius CAD4	Enraf-Nonius CAD4	Enraf-Nonius CAD4
scan method	θ–2θ	θ–2θ	θ–2θ
h,k,l limits:	−11–+11,0–18,0–16	0–18,0–19,0–12	−13–+13,0–59,0–22
2θ range, deg	4.00–45.00	4.00–50.00	4.00–50.00
scan width, deg	0.95 + 0.35 tan (θ)	0.75 + 0.35 tan (θ)	0.50 + 0.35 tan (θ)
take-off angle, deg	5.00	4.80	2.80
programs used	Enraf-Nonius SDP	Enraf-Nonius SDP	Enraf-Nonius SDP
F_{000}	1256.0	1252.0	2516.0
p factor used in weighting	0.07	0.070	0.040
no. of unique data	3654	2725	9981
data with $I > 3.0\sigma(I)$	3229	2263	5330
no. of variables	528	282	550
largest shift/esd in final cycle	0.31	0.84	0.00
R	0.033	0.048	0.035
R_w	0.044	0.062	0.040
goodness of fit	1.379	1.349	0.890

[a] Walker, N.; Stuart, D. *Acta Crystallogr., Sect. A* **1983**, *A39*, 158.

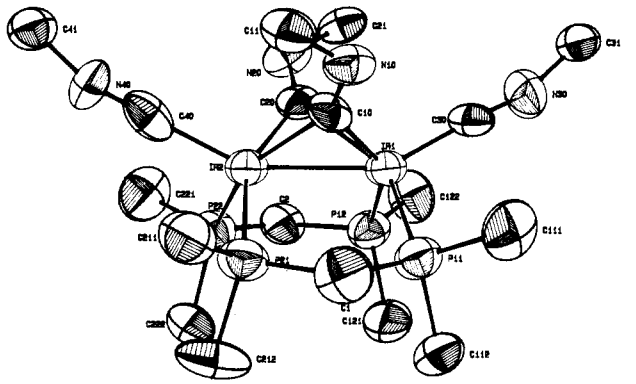

Figure 1. Molecular structure of $Ir_2(CNR)_4(dmpm)_2$ (R = 2,6-$Me_2C_6H_3$) (**1**) showing 50% probability thermal ellipsoids. For clarity, only the ipso 2,6-xylyl carbon atoms bonded to nitrogen atoms have been included.

correction for extinction was applied. The structure was solved by MULTAN–least-squares–Fourier methods and was refined to R and R_w values of 0.033 and 0.044, respectively, for 528 variables and 3229 observations with $F^2 > 3\sigma(F^2)$. Changing the enantiomer did not significantly change the R factors. An empirical absorption correction based on a series of ψ scans was applied to the data. Positional and thermal parameters and their estimated standard deviations are listed in supplementary material.

$Ir_2\{CN(BH_3)\}_2(CNR)_2(dmpm)_2$ (R = 2,6-$Me_2C_6H_3$) (2). Crystals of complex **2** were first obtained from methylene chloride/diethyl ether solution, but these were twinned. The crystal used in the X-ray study was eventually obtained by slow diffusion of diethyl ether into a THF solution containing **2**. Crystal data and collection parameters for **2** are summarized in Table I. The structure was solved by MULTAN–least-squares–Fourier methods. An empirical absorption correction based on a series of ψ scans was applied to the data. Positional and thermal parameters and their estimated deviations are listed in supplementary material.

$Ir_2\{(CNR)_2AlEt_2\}(CNR)_2(dmpm)_2$ (R = 2,6-$Me_2C_6H_3$) (3). Single crystals of **3** were obtained by slow diffusion of hexanes into a toluene solution of **3**. The crystal used for data collection was mounted in a capillary tube and sealed in place with epoxy cement. Crystal data and collection parameters for complex **3** are summarized in Table I. Three standard reflections were monitored after every 100 reflections, and no decay was noticed over the data collection. No correction for extinction was applied. The structure was solved by MULTAN–least-squares–Fourier methods. An empirical absorption correction based on a series of ψ scans was applied to the data. Positional and thermal parameters and their estimated deviations are listed in supplementary material.

Results and Discussion

Synthesis of $Ir_2(\mu\text{-}CNR)_2(CNR)_2(dmpm)_2$ (R = 2,6-$Me_2C_6H_3$) (1). Complex **1** is prepared by Na/Hg reduction of the bis(dimethylphosphino)methane (dmpm) bridged Ir(I) complex, $[Ir_2(\mu\text{-}CNR)(CNR)_4(dmpm)_2][PF_6]_2$ (R = 2,6-$Me_2C_6H_3$).[14] The net 2e$^-$ reduction is accompanied by liberation of 1 equiv of isocyanide, eq 1. A more convenient method of preparing **1** is

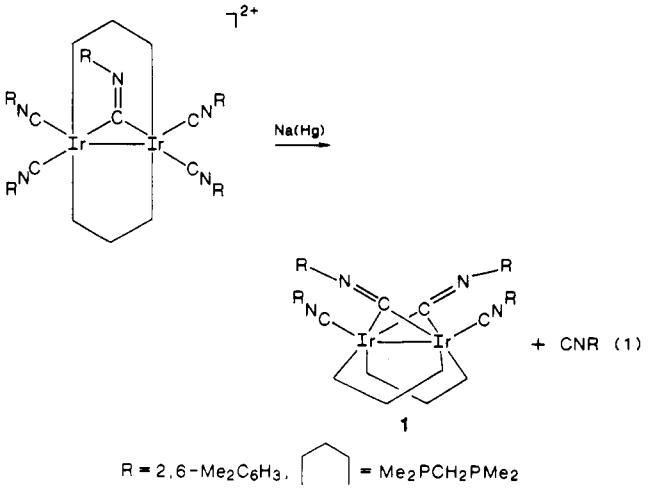

by direct reduction of a mixture of 1 equiv of $[Ir(COD)Cl]_2$, 2 equiv of dmpm, and 4 equiv of 2,6-xylyl isocyanide in benzene solution. The formation of **1** is conveniently monitored by IR spectroscopy. The terminal isocyanide bands of **1** appear at 2038

Table II. Bond Distances (Å) and Angles (deg) for Complex **1**

atom 1	atom 2	distance[a]	atom 1	atom 2	distance [a]
Ir(1)	Ir(2)	2.5998 (7)	P(12)	C(2)	1.82 (2)
Ir(1)	P(11)	2.240 (4)	P(21)	C(1)	1.81 (2)
Ir(1)	P(12)	2.399 (4)	P(22)	C(2)	1.84 (2)
Ir(1)	C(10)	2.04 (1)	N(10)	C(10)	1.29 (2)
Ir(1)	C(20)	2.20 (1)	N(10)	C(11)	1.47 (2)
Ir(1)	C(30)	1.87 (1)	N(20)	C(20)	1.24 (2)
Ir(2)	P(21)	2.264 (4)	N(20)	C(21)	1.46 (2)
Ir(2)	P(22)	2.383 (5)	N(30)	C(30)	1.15 (2)
Ir(2)	C(10)	1.98 (1)	N(30)	C(31)	1.40 (2)
Ir(2)	C(20)	2.07 (1)	N(40)	C(40)	1.17 (2)
Ir(2)	C(40)	1.98 (2)	N(40)	C(41)	1.37 (2)
P(11)	C(1)	1.86 (1)	P(21)	C(211)	1.80 (2)
P(11)	C(111)	1.89 (2)	P(21)	C(212)	1.79 (2)
P(11)	C(112)	1.84 (2)	P(22)	C(221)	1.84 (2)
P(12)	C(121)	1.85 (2)	P(22)	C(222)	1.84 (2)
P(12)	C(122)	1.80 (2)			

atom 1	atom 2	atom 3	angle[a]	atom 1	atom 2	atom 3	angle[a]
Ir(2)	Ir(1)	P(11)	94.6 (2)	P(22)	Ir(2)	C(10)	146.4 (4)
Ir(2)	Ir(1)	P(12)	95.11 (9)	P(22)	Ir(2)	C(20)	83.7 (4)
Ir(2)	Ir(1)	C(10)	48.8 (3)	P(22)	Ir(2)	C(40)	96.8 (4)
Ir(2)	Ir(1)	C(20)	50.3 (3)	C(10)	Ir(2)	C(20)	71.6 (5)
Ir(2)	Ir(1)	C(30)	151.3 (4)	C(10)	Ir(2)	C(40)	110.6 (6)
P(11)	Ir(1)	P(12)	104.0 (1)	C(20)	Ir(2)	C(40)	103.7 (5)
P(11)	Ir(1)	C(10)	88.6 (4)	Ir(1)	P(11)	C(1)	112.0 (6)
P(11)	Ir(1)	C(20)	144.9 (4)	Ir(1)	P(12)	C(2)	110.8 (5)
P(11)	Ir(1)	C(30)	104.8 (5)	Ir(2)	P(21)	C(1)	109.0 (5)
P(12)	Ir(1)	C(10)	143.0 (3)	Ir(2)	P(22)	C(2)	109.6 (5)
P(12)	Ir(1)	C(20)	83.3 (3)	C(10)	N(10)	C(11)	121 (1)
P(12)	Ir(1)	C(30)	100.4 (4)	C(20)	N(20)	C(21)	122 (1)
C(10)	Ir(1)	C(20)	67.9 (5)	C(30)	N(30)	C(31)	162 (2)
C(10)	Ir(1)	C(30)	109.9 (5)	C(40)	N(40)	C(41)	165 (2)
C(20)	Ir(1)	C(30)	107.6 (6)	Ir(1)	C(10)	Ir(2)	80.7 (5)
Ir(1)	Ir(2)	P(21)	98.5 (2)	Ir(1)	C(10)	N(10)	134 (2)
Ir(1)	Ir(2)	P(22)	96.7 (2)	Ir(2)	C(10)	N(10)	145 (1)
Ir(1)	Ir(2)	C(10)	50.6 (5)	Ir(1)	C(20)	Ir(2)	74.8 (5)
Ir(1)	Ir(2)	C(20)	55.0 (4)	Ir(1)	C(20)	N(20)	142 (1)
Ir(1)	Ir(2)	C(40)	153.1 (4)	Ir(2)	C(20)	N(20)	143 (1)
P(21)	Ir(2)	P(22)	102.9 (2)	Ir(1)	C(30)	N(30)	175 (1)
P(21)	Ir(2)	C(10)	90.7 (4)	Ir(2)	C(40)	N(40)	179 (2)
P(21)	Ir(2)	C(20)	153.3 (4)	P(11)	C(1)	P(21)	116 (2)
P(21)	Ir(2)	C(40)	101.1 (5)	P(12)	C(2)	P(22)	115.3 (9)

[a] Numbers in parentheses are estimated standard deviations in the least significant digits.

and 1996 cm^{-1} (KBr). These occur at extremely low energies for terminal isocyanides in general and are approximately 100 cm^{-1} lower than the corresponding bands in the spectrum of $[Ir_2(\mu\text{-}CNR)(CNR)_4(dmpm)_2][PF_6]_2$ (R = 2,6-$Me_2C_6H_3$).[14] The bridging isocyanides of **1** appear in the IR at ν(CN) = 1600 and 1564 cm^{-1} (KBr). The low ν(CN) stretching frequencies exhibited by **1** reflect the rich electron density of a zero-valent, d^9–d^9 binuclear transition-metal complex with strongly electron-donating dmpm ligands. Not surprisingly, complex **1** is highly air sensitive and very reactive toward a number of small molecules, including carbon dioxide.[16] Complex **1** is soluble in benzene, toluene, and THF and has been characterized by ^1H and $^{31}P\{^1H\}$ NMR studies, as well as by an X-ray diffraction study described below. Integration of the ^1H NMR spectrum of **1** reveals two dmpm and four 2,6-xylyl isocyanide ligands, which, together with analytical data, are consistent with the formula indicated in eq 1. Complex **1** is among only a few examples of zero-valent iridium complexes containing isocyanide ligands. To our knowledge, the only other structurally characterized Ir(0) isocyanide complexes are the tetranuclear clusters, $Ir_4(CO)_{12-x}(CNR)_x$ (R = Bu^t, x = 1–6; R = Me, x = 1–4).[17,18]

Structure of $Ir_2(CNR)_4(dmpm)_2$ (R = 2,6-$Me_2C_6H_3$) (1). The structure of **1** was determined by X-ray diffraction. An ORTEP drawing of the molecular structure of **1** is presented in Figure 1. Crystal data are summarized in Table I. Bond distances and angles are given in Table II. Complex **1** exhibits a *cis,cis*-$M_2(dmpm)_2$ framework. The overall structure is analogous to and isoelectronic with the bridging form of $Co_2(CO)_8$.[19] The structure consists of two approximately square-pyramidally coordinated Ir(0) centers, separated by 2.5998 (7) Å.[20] Each iridium atom lies 0.48–0.58 Å out of the essentially square plane formed by the carbon atoms of the two bridging isocyanide ligands and the two cis-dmpm phosphorus atoms coordinated to each iridium atom. The dihedral angle between these two equatorial planes is 63.5°. $M_2(\mu\text{-}L)_2L_6$ structures of this type are in fact quite common for zero-valent complexes of the cobalt triad. Other than $Co_2(CO)_8$,[19] several other isoelectronic M_2L_8 complexes have been structurally characterized. The isocyanide complexes $Co_2(CNBu^t)_8$[21] and

(16) Wu, J.; Fanwick, P. E.; Kubiak, C. P. *Organometallics* **1987**, *6*, 1507.
(17) (a) Shapley, J. R.; Stuntz, G. F.; Churchill, M. R.; Hutchinson, J. P. *J. Chem. Soc., Chem. Commun.* **1979**, 219. (b) Churchill, M. R.; Hutchinson, J. P. *Inorg. Chem.* **1979**, *18*, 2451.
(18) The binuclear iridium(0) isocyanide complex, $Ir_2(CNR)_8$ (R = 2,6-$Me_2C_6H_3$), was prepared recently in this laboratory: Burkholder, S. P. M.S. Thesis, Purdue University, May 1987.
(19) Sumner, G. G.; Klug, H. P.; Alexander, L. E. *Acta Crystallogr.* **1964**, *17*, 732.
(20) Iridium–iridium single bond length varies in the range of 2.524–3.017 Å. See: (a) Cotton, F. A.; Lahuerta, P.; Sanau, M.; Schwotzer, W. *J. Am. Chem. Soc.* **1985**, *107*, 8284. (b) Sutherland, B. R.; Cowie, M. *Organometallics* **1985**, *4*, 1801. (c) Sutherland, B. R.; Cowie, M. *Inorg. Chem.* **1984**, *23*, 2324. (d) Cowie, M.; Sutherland, B. R. *Organometallics* **1984**, *3*, 1869. (e) Mague, J. T.; Klein, C. L.; Majeste, R. J.; Steves, E. D. *Organometallics* **1984**, *3*, 1860. (f) Angoletta, M.; Bellon, P.; Demartin, F. *J. Organomet. Chem.* **1984**, *267*, 199. (g) Sansoni, M. *J. Organomet. Chem.* **1981**, *204*, C10. (h) Kubiak, C. P.; Woodcock, C.; Eisenberg, R. *Inorg. Chem.* **1980**, *19*, 2733. (i) Churchill, M. R.; Hutchinson, J. P. *Inorg. Chem.* **1978**, *17*, 3528. (j) Stuntz, G. F.; Shapley, J. R.; Pierpoint, C. G. *Inorg. Chem.* **1978**, *17*, 2596. (k) Heveldt, P. F.; Johnson, B. F. G.; Lewis, J.; Raithby, P. R.; Sheldrick, G. M. *J. Chem. Soc., Chem. Commun.* **1978**, 340. (l) Albano, V.; Bellon, P.; Scatturin, V. *Chem. Commun.* **1967**, 730. (m) Cotton, F. A.; Poli, R. *Polyhedron* **1987**, *6*, 1625.

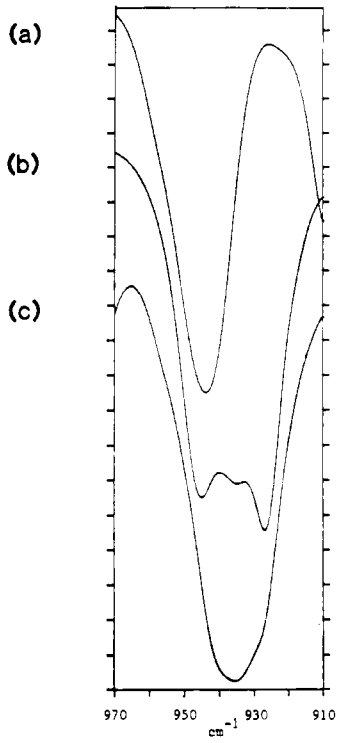

Figure 2. FTIR absorption band features in the ν(PC) region for a *trans,trans*-$M_2(dmpm)_2$ structure $[Ir_2(CNR)_5(dmpm)_2][PF_6]_2$[14] (a) and the *cis,cis*-$M_2(dmpm)_2$ complexes **1** (b) and **3** (c).

$Ir_2(CNR)_8$ (R = 2,6-$Me_2C_6H_3$)[18] possess similar structures without bridging diphosphines. This structural framework can be supported by one or two diphosphines or diarsines. For example, $Co_2(CO)_6$(ffars) (ffars = 1,2-bis(dimethylarsino)tetrafluorocyclobutene),[22] possesses a single diarsine spanning the metal centers. Complex **1** is a bis(diphosphine)-supported system of structure II and is thus one of several examples reported recently in which two bridging diphosphine ligands support two metals in a cradle-type cis,cis conformation.[23]

A noteworthy feature of the structure of **1** is a short nonbonded C···C separation between the bridging isocyanide carbon atoms. The C10···C20 distance is 2.37 (2) Å, substantially shorter than the sum of van der Waals radii for aromatic carbon atoms, 3.70 Å.[24] The short μ-isocyanide C···C distance is especially interesting for the possibilities it offers to study C–C bond formation at binuclear reaction sites. The two μ-isocyanide ligands are distinctly bent, ∠C10–N10–C11 = 121 (1)° and ∠C20–N20–C21 = 122 (1)°, relative to the terminal isocyanides, ∠C30–N30–C31 = 162 (2)° and ∠C40–N40–C41 = 165 (2)°. The orientation of the 2,6-xylyl groups of the bridging ligands is anti. These factors render the nitrogen atoms of the bridging ligands accessible to electrophilic reagents.

Correlation of ν(PC) Absorption Band Shape and $M_2(dmpm)_2$ Geometry. A structurally sensitive IR probe emerged from our studies of dmpm-bridged binuclear complexes. Sufficient structural and spectroscopic data now exist to distinguish *cis,cis*-$M_2(dmpm)_2$ frameworks characteristic of cradle-type complexes from the *trans,trans*-$M_2(dmpm)_2$ frameworks of A-frame, face-to-face $M_2(dmpm)_2L_4$, and related complexes. In the ν(PC) region, **1** exhibits two bands at 945 and 933 cm^{-1} (KBr). In contrast its trans,trans precursor, $[Ir_2(CNR)_5(dmpm)_2][PF_6]_2$[14] (R = 2,6-$Me_2C_6H_3$), has only one sharp ν(PC) band at 943 cm^{-1} (KBr) in its FTIR spectrum. This correlation between ν(PC) band features in the 920–950-cm^{-1} region and $M_2(dmpm)_2$ geometry has proven to be general: (i) two or more strong bands of approximately equal intensity, as illustrated by complex **1** or **2** (Figure 2b) or a broad band as observed for complex **3** (Figure 2c) indicates a cradle-type *cis,cis*-$M_2(dmpm)_2$ geometry; (ii) a single sharp band, normally at ~943 cm^{-1}, indicates a *trans,trans*-$M_2(dmpm)_2$ geometry (Figure 2a), as illustrated by $[Ir_2(CNR)_5(dmpm)_2][PF_6]_2$ and several other *trans,trans*-$M_2(dmpm)_2$ complexes including $Pd_2Br_2(dmpm)_2$,[25a] $Pd_2(\mu\text{-CO})Cl_2(dmpm)_2$,[25b] $[Ir_2(\mu\text{-}CH_2)(CO)_4][SO_3CF_3]$,[26] $[Ir_2(\mu\text{-}CH_3)(CO)_2(dmpm)_2][SO_3CF_3]$,[26] and $[Ir_2(\mu\text{-H})_2(CNR)_4(dmpm)_2][PF_6]_2$.[14]

Reaction of BH_3·THF with the Bridging Isocyanide Ligands of 1. The reaction of **1** with BH_3·THF was carried out to investigate the potential coupling of the μ-isocyanides via conversion of the isocyanides to their aminocarbyne form. The nitrogen atoms of the bridging isocyanide ligands of complex **1** are indeed basic in the Lewis sense. As a result, **1** reacts with Lewis acids to form the corresponding N adducts. This reaction has precedence in our studies of the μ-isocyanide ligands of Ni(0) complexes.[11] In the earlier studies, a μ-CN(H)Me$^+$ complex was structurally characterized and compared to its parent μ-CNMe complex. The N protonation of the μ-isocyanide was found to result in significant ground-state aminocarbyne character.[11a] We anticipated that a bis(aminocarbyne) derivative of **1** might further react to give the corresponding coupled alkyne.

Complex **1** reacts quantitatively with 2 equiv of BH_3·THF in benzene to give a compound of stoichiometry $Ir_2(\mu\text{-CNR-}(BH_3))_2(CNR)_2(dmpm)_2$, (R = 2,6-$Me_2C_6H_3$) (**2**). Complex **2** is obtained as a white solid, which is analytically pure, and has been characterized by IR and ^1H and $^{31}P\{^1H\}$ NMR. The presence of two strong ν(PC) bands at 949 and 933 cm^{-1} (KBr) suggests that **2** has a cradle-type structure similar to **1** (vide supra). The IR spectrum of **2** provides considerable evidence for N-adduct formation involving the μ-isocyanides of **1**. Upon reaction of **1** with BH_3·THF, the bridging ν(CN) bands at 1600 and 1564 cm^{-1} shift to 1520 and 1500 cm^{-1}. The shifts in the ν(CN) bands of the bridging isocyanide ligands are consistent with a decrease in the C=N bond order, upon reaction with BH_3·THF. Our studies of complexation of Lewis acids to μ-isocyanide ligands are similar in several respects to the studies of Shriver and co-workers on Lewis acid adducts of μ-carbonyls.[27] There is, however, an important distinction. The reaction of **1** ($\nu(CN)_{bridging}$ = 1600, 1564 cm^{-1}) with 2 equiv of BH_3 produces **2** ($\nu(CN)_{bridging}$ = 1520, 1500 cm^{-1}) and reduces $\nu(CN)_{bridging}$ by ≃70 cm^{-1}. The reaction $[FeCp(CO)_2]_2$ ($\nu(CO)_{bridging}$ = 1800 cm^{-1}) with 2 equiv of AlR_3 produces $[FeCp(CO(AlR_3))(CO)]_2$ ($\nu(CO)_{bridging}$ = 1700 cm^{-1}). Although the degree of change of $\nu(CN)_{bridging}$ and $\nu(CO)_{bridging}$ induced by Lewis acid complexation is similar, the net multiple C–E (E = NR, O) bond character in **2** is expected to be significantly less compared to $[FeCp(CO(AlR_3))(CO)]_2$ since ν(C–E) (E = NR, O) is less by ≃200 cm^{-1}. Note ν(CN) = 2109 cm^{-1} for 2,6-Me_2–C_6H_3–NC, c.f. ν(CO) = 2143 cm^{-1} for CO(g). In general, complexes with bridging isocyanide ligands can be viewed in terms of μ-isocyanide (a) and μ-amidocarbyne (b) canonical

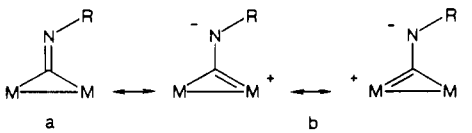

(21) Corroll, W. E.; Green, M.; Galas, A. M.; Murray, M.; Turney, T. W.; Welch, A. J.; Woodward, P. *J. Chem. Soc., Dalton Trans.* **1980**, 80.

(22) (a) Crow, J. P.; Cullen, W. R.; Harrison, W.; Trotter, J. *J. Am. Chem. Soc.* **1970**, *92*, 6339. (b) Harrison, W.; Trotter, J. *J. Chem. Soc. A* **1971**, 1607.

(23) A few other complexes also possess a similar "cradle" structure. See: (a) Einspahr, H.; Donohue, J. *Inorg. Chem.* **1974**, *13*, 1839. (b) Karsch, H. H.; Milewski-Mahrla, B. *Angew. Chem., Int. Ed. Engl.* **1981**, *20*, 814. (c) Karsch, H. H.; Milewski-Mahrla, B.; Besenhard, J.; Hofmann, P.; Stauffert, P.; Albright, T. A. *Inorg. Chem.* **1986**, *25*, 3811. (d) Osborn, J. A.; Stanley, G. G.; Bird, P. H. *J. Am. Chem. Soc.* **1988**, *110*, 2117. (e) Berry, D. H.; Eisenberg, R. *Organometallics* **1987**, *6*, 1796. (f) Cotton, F. A.; Dunbar, K. R.; Verbruggen, M. G. *J. Am. Chem. Soc.* **1987**, *109*, 5498.

(24) Weast, R. C., Ed. *Handbook of Chemistry and Physics*, 50th ed.; CRC: Cleveland, OH, 1970; p D-178.

(25) (a) Kullberg, M. L.; Lemke, F. R.; Powell, D. R.; Kubiak, C. P. *Inorg. Chem.* **1985**, *24*, 3589. (b) Kullberg, M. L.; Kubiak, C. P. *Organometallics* **1984**, *3*, 632; *Inorg. Chem.* **1986**, *25*, 26.

(26) Reinking, M. K.; Fanwick, P. E.; Kubiak, C. P. *Angew. Chem., Int. Ed. Engl.*, in press.

(27) Shriver, D. F.; Alich, A. *J. Organomet. Chem.* **1975**, *94*, 259.

Table III. Bond Distances (Å) and Angles (deg) for Complex **2**

atom 1	atom 2	distance[a]	atom 1	atom 2	distance[a]
Ir	Ir	2.589 (2)	C(2)	C(3)	1.41 (2)
Ir	P(1)	2.341 (4)	C(2)	C(7)	1.36 (3)
Ir	P(2)	2.328 (4)	C(3)	C(4)	1.39 (2)
Ir	C(1)	2.03 (1)	C(3)	C(8)	1.51 (3)
Ir	C(1)	2.01 (2)	C(4)	C(5)	1.43 (3)
Ir	C(30)	1.99 (2)	C(5)	C(6)	1.40 (3)
P(1)	C(B)	1.80 (2)	C(6)	C(7)	1.45 (3)
P(1)	C(11)	1.81 (2)	C(7)	C(9)	1.58 (3)
P(1)	C(12)	1.87 (2)	C(32)	C(33)	1.35 (2)
P(2)	C(B)	1.91 (2)	C(32)	C(37)	1.45 (3)
P(2)	C(21)	1.83 (2)	C(33)	C(34)	1.44 (3)
P(2)	C(22)	1.84 (2)	C(33)	C(38)	1.53 (4)
N(2)	C(1)	1.34 (2)	C(34)	C(35)	1.38 (3)
N(2)	C(2)	1.50 (3)	C(35)	C(36)	1.44 (3)
N(2)	B	1.59 (3)	C(36)	C(37)	1.39 (3)
N(31)	C(30)	1.11 (2)	C(37)	C(39)	1.51 (3)
N(31)	C(32)	1.43 (2)			

atom 1	atom 2	atom 3	angle[a]	atom 1	atom 2	atom 3	angle[a]
Ir	Ir	P(1)	95.2 (2)	C(B)	P(2)	C(21)	101.6 (9)
Ir	Ir	P(2)	97.6 (2)	C(B)	P(2)	C(22)	100.8 (8)
Ir	Ir	C(1)	49.9 (4)	C(21)	P(2)	C(22)	102.1 (8)
Ir	Ir	C(1)	50.5 (4)	C(1)	N(2)	C(2)	119 (1)
Ir	Ir	C(30)	155.6 (4)	C(1)	N(2)	B	127 (2)
P(1)	Ir	P(2)	101.3 (1)	C(2)	N(2)	B	114 (1)
P(1)	Ir	C(1)	145.2 (5)	C(30)	N(31)	C(32)	169 (2)
P(1)	Ir	C(1)	86.3 (5)	Ir	C(1)	Ir	79.6 (6)
P(1)	Ir	C(30)	99.7 (4)	Ir	C(1)	N(2)	140 (1)
P(2)	Ir	C(1)	84.9 (5)	Ir	C(1)	N(2)	141 (1)
P(2)	Ir	C(1)	148.0 (4)	N(2)	C(2)	C(3)	119 (1)
P(2)	Ir	C(30)	98.3 (5)	N(2)	C(2)	C(7)	120 (2)
C(1)	Ir	C(1)	72.2 (8)	C(3)	C(2)	C(7)	121 (2)
C(1)	Ir	C(30)	113.5 (6)	C(2)	C(3)	C(4)	120 (2)
C(1)	Ir	C(3)	111.0 (6)	C(2)	C(3)	C(8)	123 (2)
Ir	P(1)	C(B)	11.3 (7)	C(4)	C(3)	C(8)	117 (2)
Ir	P(1)	C(11)	124.9 (8)	C(3)	C(4)	C(5)	119 (2)
Ir	P(1)	C(12)	118.8 (7)	C(4)	C(5)	C(6)	120 (2)
C(B)	P(1)	C(11)	99 (1)	C(5)	C(6)	C(7)	119 (2)
C(B)	P(1)	C(12)	99.6 (8)	C(2)	C(7)	C(6)	120 (2)
C(11)	P(1)	C(12)	99.1 (9)	C(2)	C(7)	C(9)	127 (2)
Ir	P(2)	C(B)	109.2 (6)	C(6)	C(7)	C(9)	113 (2)
Ir	P(2)	C(21)	124.9 (6)	P(1)	C(B)	P(2)	114.1 (9)
Ir	P(2)	C(22)	115.0 (7)	Ir	C(30)	N(31)	175 (1)

[a] Numbers in parentheses are estimated standard deviations in the least significant digits.

structures. For low-valent group VIII metal complexes, the carbyne forms appear to become increasingly important and contribute to facile N alkylation or carboxylation.[11] Complexation of the isocyanide N atoms of **1** with BH_3 further increases the carbyne character of the bridging ligands. The μ-carbyne ligands resulting from the reaction of **1** with BH_3, however, do not couple to produce an alkyne, as is evident from the structural study described below.

Structure of $Ir_2(\mu\text{-}CN(BH_3)R)_2(CNR)_2(dmpm)_2$ (R = 2,6-$Me_2C_6H_3$) (2). The structure of the BH_3 adduct, **2** was determined by X-ray diffraction. Crystal data for **2** are summarized in Table I. An ORTEP drawing of the molecular structure of **2** is presented in Figure 3. Bond distances and angles are given in Table III. The structure of **2** clearly shows that a BH_3 group has been added to each of the two bridging isocyanide ligands. The molecule possesses crystallographic C_2 symmetry with the 2-fold axis bisecting the Ir–Ir vector. The overall structure of complex **2** is essentially identical with the cradle-type structure of **1**. Bond distances and angles in the $Ir_2(dmpm)_2$ core of **2** deviate by averages of only 0.02 (2) Å and 2.0 (9)°, respectively, compared to **1**. The Ir–Ir separation is 2.589 (2) Å, slightly shorter than that of **1**. The molecular structure of **2** suggests partial carbyne character for the bridging $CN(BH_3)R$ groups. The bridging ligand C–N distances increase from 1.24 (2) and 1.29 (2) Å for the bis(μ-isocyanide), **1**, to 1.34 (2) Å for the bis(μ-aminocarbyne), **2**. The average iridium to bridging carbon distances for **1** are longer than those for **2**, but they do not differ within the 3σ confidence level, 2.07 (9) Å for **1** vs 2.02 (1) Å for **2**. This results from the asymmetry of the iridium to bridging carbon bond lengths

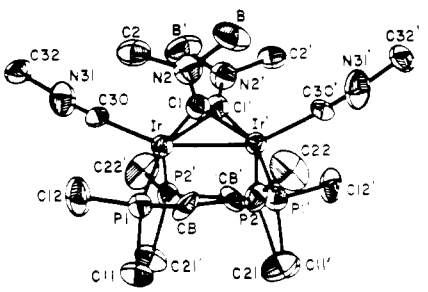

Figure 3. Molecular structure of $Ir_2\{CN(BH_3)R\}_2(CNR)_2(dmpm)_2$ (R = 2,6-$Me_2C_6H_3$) (**2**) showing 50% probability thermal ellipsoids. For clarity, only the ipso 2,6-xylyl carbon atoms bonded to nitrogen atoms have been included.

of **1** from Ir2–C10, 1.98 (1) Å, to Ir1–C20, 2.20 Å. The B–N distance of 1.59 (3) Å in **2** is somewhat longer than a typical B–N single bond, 1.42 (1) Å.[28] A comparison of the inner cores of

(28) A B–N single bond length is typically 1.42 (1) Å. See: *Handbook of Chemistry and Physics*, 57th ed.; CRC: Cleveland, OH, 1977; p F-217.

(29) (a) King, R. B.; Harmon, C. A. *Inorg. Chem.* **1976**, *15*, 879. (b) Cash, G. G.; Pettersen, R. C.; King, R. B. *J. Chem. Soc., Chem. Commun.* **1977**, 30.

(30) Cotton, F. A.; Adams, R. D. *Inorg. Chem.* **1974**, *13*, 249.

(31) In the liquid state, the lower aluminum alkyls such as $AlEt_3$ exist as dimers. See: (a) Cotton, F. A.; Wilkinson, G. *Advanced Inorganic Chemistry*, 4th ed.; John Wiley: New York, 1980; p 343. (b) Moore, J. W.; Sanders, D. A.; Scherr, P. A.; Glick, M. D.; Oliver, J. P. *J. Am. Chem. Soc.* **1971**, *93*, 1035.

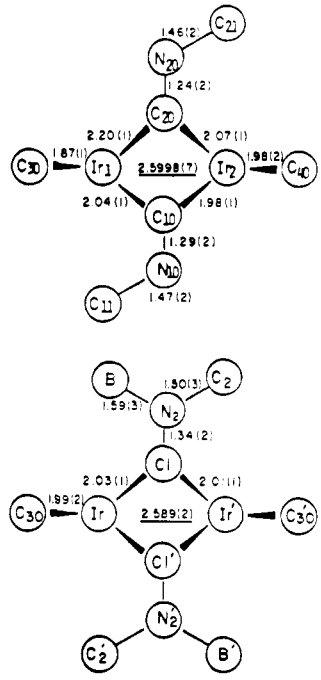

Figure 4. Comparison of the inner coordination geometries of $Ir_2(CNR)_4(dmpm)_2$ (R = 2,6-$Me_2C_6H_3$) (**1**) and $Ir_2\{CN(BH_3)R\}_4(dmpm)_2$ (R = 2,6-$Me_2C_6H_3$) (**2**).

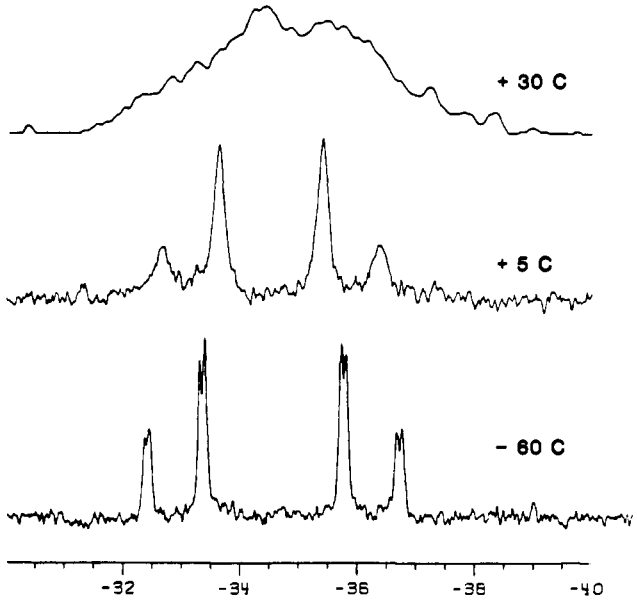

Figure 5. Variable $^{31}P\{^1H\}$ NMR spectra of $Ir_2(CNR)_4(dmpm)_2$ (R = 2,6-$Me_2C_6H_3$) (**1**) in toluene-d_8.

1 and **2** is presented in Figure 4.

A key finding from the BH_3 addition reaction is that the conversion of the bis(μ-isocyanide), **1**, to the bis(μ-aminocarbyne), **2**, is not accompanied by carbon–carbon bond formation between the carbyne groups. The aminocarbyne nonbonded C···C distance in **2**, 2.39 (2) Å, is shorter than the sum of van der Waals radii, but is slightly longer than that found in **1**. The distance most certainly is not consistent with C···C bond formation. We note that numerous examples of μ-alkyne $M_2(\mu\text{-}R_2C_2)L_6$ complexes related to **2** do exist. In particular, Berry and Eisenberg recently reported a μ-alkyne dirhodium complex, $Rh_2(PhCCPh)(CO)_2(dppm)_2$, with the cradle-type structure, IV.[33] The bis(μ-isocyanide), II, bis(μ-aminocarbyne), III, and μ-alkyne, IV, provide

(32) Initial addition of 1, 4, or 6 equiv of $AlEt_3$ led to unclean ^{31}P spectra, and the final product could not be obtained.

(33) Berry, D. H.; Eisenberg, R. *Organometallics* **1987**, *6*, 1796.

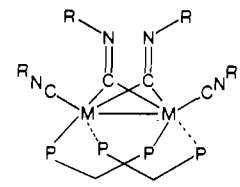

II

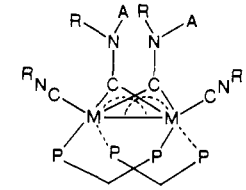

III

1: M = Ir, R = 2,6-$Me_2C_6H_3$ **2**: M = Ir, R = 2,6-$Me_2C_6H_3$, A = BH_3

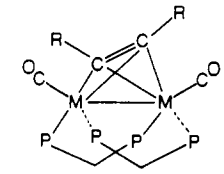

IV

M = Rh, R = Ph

a plausible set of limiting structures for the coupling of isocyanides via aminocarbyne intermediates. An interesting comparison can be drawn between **2** and an isoelectronic iron complex, $Fe_2(\mu\text{-}C{=}NEt_2)_2(CO)_6$.[29] The diiron aminocarbyne is formed by rupture of the C≡C bond of bis(diethylamino)ethyne, eq 2. This rep-

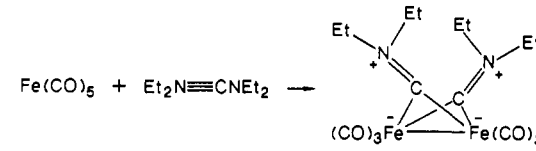

(2)

resents the reverse of our intended Lewis acid promoted carbon–carbon bond formation. Clearly, the relative stabilities of μ-alkyne vs bis(μ-carbyne) limiting structures largely determine whether C≡C bonds are made or broken.

^{31}P NMR Studies of 1 and 2. The ^{31}P NMR spectrum of **1** at room temperature consists of one broad signal. In contrast, the spectrum of **2** at room temperature clearly shows an AA′BB′ pattern. As the temperature is gradually cooled, the ^{31}P NMR spectrum of **1** also becomes an AA′BB′ pattern. At −60 °C, the spectrum of **1** appears qualitatively similar to that of **2** at room temperature. The ^{31}P NMR spectra of **1** over the temperature range −60 to +30 °C are presented in Figure 5. From the structural comparison of **1** and **2**, it is evident that **2** is sterically more crowded than **1** due to complexation of BH_3 groups. Computer simulation of the 25 °C $^{31}P\{^1H\}$ NMR spectrum of **2** and the −60 °C spectrum of **1** indicates that in both cases the dominant coupling constant is $J(P_A\text{–}P_B)$ and that the calculated values are identical ($J(P_A\text{–}P_B)$ = 116 Hz). The dynamic process, evident in the $^{31}P\{^1H\}$ NMR spectra of **1** is believed to be interconversion of syn and anti isomers, eq 3. A similar interconversion has been observed in the case of $Cp_2Fe_2(CO)_2(CNMe)_2$.[30]

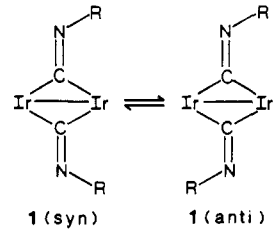

(3)

1 (syn) **1** (anti)

As the temperature is decreased, rates of the syn ⇄ anti conversion are slowed, until the limiting spectrum of the more stable isomer is observed. It is the anti isomer of **1** which appears to be more stable. Complex **2** exhibits no syn ⇄ anti exchange process in solution, and we assume that the static solution structure corresponds to the solid-state structure of 2, which is anti. On the basis of the extremely similar $^{31}P\{^1H\}$ NMR AA′BB′ coupling data for **2** at room temperature and **1** at −60 °C, we assign an overall anti configuration to the μ-isocyanide aryl groups at low temperature. This corresponds to the solid-state structure of **1**.

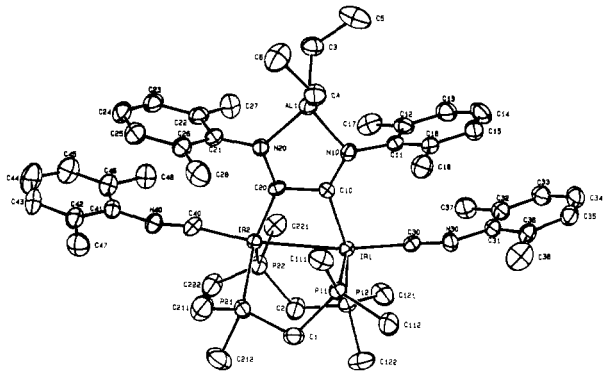

Figure 6. Molecular structure of $Ir_2\{C_2(NR)_2AlEt_2\}(CNR)_2(dmpm)_2$ (R = 2,6-$Me_2C_6H_3$) (**3**) showing 30% probability thermal ellipsoids.

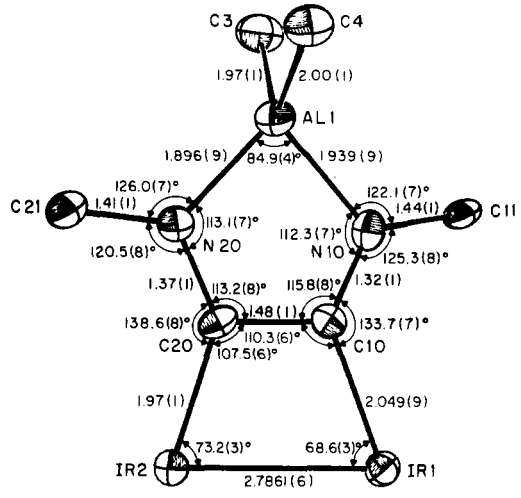

Figure 7. Skeletal view of **3** with selected bond distances and angles.

Al_2Et_6-Promoted Carbon–Carbon Bond Formation between the μ-Isocyanides of 1. Reaction of 1 with Al_2Et_6 and Formation of 3. Additon of 1 equiv of neat Al_2Et_6[31] to a toluene solution containing **1** at 25 °C caused an immediate color change from light yellow to dark brown. Although the terminal isocyanide ν(CN) bands did not change noticeably, the bridging isocyanide ν(CN) bands diminished in intensity and a new band at $\simeq$1520 cm^{-1} appeared. The $^{31}P\{^1H\}$ NMR spectrum showed the replacement of the broad signal corresponding to **1** at δ −34.7 ppm by a doublet of triplets centered at δ −38.6 and −47.8 ppm (J = 40 Hz).[32] These observations are consistent with an asymmetric adduct resulting from the addition of one $AlEt_3$ molecule to one of the bridging isocyanide ligands. A second slower reaction ensued, and after 24 h, an intense red-purple color developed and <1 equiv of C_2H_4 and <0.25 equiv of C_2H_6 were detected by gas chromatography. The product was obtained as dark red-purple crystals by slow diffusion of hexanes into the toluene reaction mixture. The isolated material has the stoichiometry $Ir_2(CNR)_4(AlEt_2)(dmpm)_2$ (R = 2,6-$Me_2C_6H_3$) (**3**). The IR spectrum of **3** exhibits two terminal isocyanide ν(CN) bands at 2047 and 1996 cm^{-1}. These are quite similar to the corresponding ν(CN) bands of **1**. The similarity between the isocyanide ν(CN) data for **1** and **3** suggests that no change in the formal oxidation of Ir(0) has occurred. The μ-isocyanide bands of **1**, however, are shifted significantly from 1600, 1656 cm^{-1} to below 1440 cm^{-1} for **3**.[15] A broad ν(PC) dmpm band at 935 cm^{-1} is consistent with a *cis,cis*-$Ir_2(dmpm)_2$ framework for **3**. Complex **3** is also paramagnetic. Together, these observations suggest that **3** can be viewed as the product of the addition of a neutral $^{\bullet}AlEt_2$ radical to the μ-isocyanide ligands of **1**.

Structure of $Ir_2(CNR)_4(AlEt_2)(dmpm)_2$(R = 2,6-$Me_2C_6H_3$) (3). The molecular structure of **3** is shown in Figure 6. Crystal data are summarized in Table I. Bond distances and angles are given in Table IV. A skeletal view with selected bond distances and angles is presented in Figure 7. The $Ir_2(dmpm)_2$ framework of

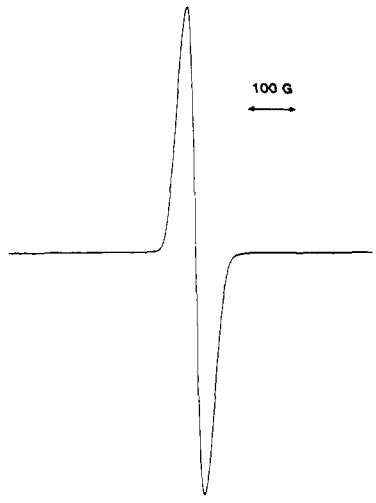

Figure 8. EPR powder spectrum of $Ir_2\{C_2(NR)_2AlEt_2\}(CNR)_2(dmpm)_2$ **3** at −150 °C.

3 has a cis,cis-dmpm configuration that is similar to **1**. The most significant feature of the structure is the coupling of the two bridging isocyanide ligands and their annulation with an $AlEt_2$ fragment. The C10–C20 distance of 1.48 (1) Å is intermediate between typical values for C–C single and double bonds. The structure conforms to the "1,2-demetalated olefin" or parallel mode of alkyne coordination to two metals.[40] This is in contrast to the parent complex **1**, and to many other known binuclear alkyne complexes including $Rh_2(PhCCPh)(CO)_2(dppm)_2$,[33] $Co_2(RCCR)(CO)_6$ (R = ^{t}Bu,[34] Ph[35]), $Co_2(HCCH)(CO)_4(PPh_3)_2$,[36] $Co_2(PhCCPh)(CO)_4(dppm)$,[37] $Co_2(PhCCPh)(CO)_2(Cp_2ArCH_2ArPh_2)_2$,[34] $Rh_2(PhCCPh)(PF_3)_4(PPh_3)_2$,[38] and $Ir_2(HCCPh)(CO)_4(PPh_3)_2$,[39] in which the vector formed by the bridging carbon atoms is perpendicular to the M–M bond.[40,41] Complex **3** also differs from the known binuclear alkyne complexes that exhibit 1,2-dimetalated olefin structures. The typical 1,2-dimetalated olefin complex is of the A-frame type structure without a metal–metal bond.[42,43] Complex **3** possesses a cradle structure and an apparent metal–metal bond, d(Ir–Ir) = 2.7861 (6) Å.

In the five-membered AlN_2C_2 ring of **3**,[44] each N atom exhibits bond angles consistent with sp^2 hybridization. The Al–N–C angles are constrained somewhat to an average of 112.7° in the five-membered ring. The Al atom exhibits bond angles that reflect sp^3 hybridization. The Al–N bond lengths of 1.939 (9) and 1.896 (9) Å are extremely long and short, respectively, for known Al–N bond distances (1.937 (5)–1.902 (4) Å.[45] The relatively acute

(34) Cotton, F. A.; Jamerson, J. D.; Stults, B. R. *J. Am. Chem. Soc.* **1976**, *98*, 1774.
(35) Sly, W. G. *J. Am. Chem. Soc.* **1959**, *81*, 18.
(36) Bonnett, J.-J.; Mathieu, R. *Inorg. Chem.* **1978**, *17*, 1973.
(37) Bird, P. H.; Fraser, A. R.; Hall, D. N. *Inorg. Chem.* **1977**, *16*, 1923.
(38) (a) Bennett, M. A.; Johnson, R. N.; Robertson, G. B.; Turney, T. W.; Whimp, P. O. *J. Am. Chem. Soc.* **1972**, *94*, 6540; (b) *Inorg. Chem.* **1976**, *15*, 97.
(39) Angoletta, M.; Bellon, P. L.; Demartin, F.; Sansoni, M. *J. Organomet. Chem.* **1981**, *208*, C12.
(40) Hoffman, D. M.; Hoffmann, R.; Fisel, C. R. *J. Am. Chem. Soc.* **1982**, *104*, 3858, and references therein.
(41) From a theoretical calculation, a perpendicular structure would be expected for **3** while a parallel structure would be expected for an A-frame complex where two diphosphine ligands are trans to each other. See: Reference 40.
(42) Cowie, M.; Dickson, R. S. *Inorg. Chem.* **1981**, *20*, 2682.
(43) Cowie, M.; Southern, T. G. *J. Organomet. Chem.* **1980**, *193*, C46.
(44) A unit similar to this one has been reported for $Cp^*_2Zr(CO)_4Fe_2Cp_2$ (Cp^* = C_5Me_5, Cp = C_5H_5). See: Reference 4a.
(45) (a) Hitchcock, P. B.; Smith, J. D.; Thomas, K. M. *J. Chem. Soc., Dalton Trans.* **1974**, 1433. (b) Amirkhalili, S.; Hitchcock, P. B.; Smith, J. D. *Ibid.* **1979**, 1206. (c) Piero, G. D.; Cesari, M.; Dozzi, G.; Mazzei, A. *J. Organomet. Chem.* **1977**, *129*, 281. (d) Piero, G. D.; Cesari, M.; Perego, G.; Cucinella, S.; Cernia, E. *Ibid.* 289. (e) Piero, G. D.; Cesari, M.; Cucinella, S.; Mazzei, A. *Ibid.* **1977**, *137*, 265.

Table IV. Bond Distances (Å) and Angles (deg) for Complex **3**

atom 1	atom 2	distance[a]	atom 1	atom 2	distance[a]
Ir(1)	Ir(2)	2.7861 (6)	P(22)	C(221)	1.84 (1)
Ir(1)	P(11)	2.328 (3)	P(22)	C(222)	1.84 (1)
Ir(1)	P(12)	2.313 (3)	Al(1)	N(10)	1.939 (9)
Ir(1)	C(10)	2.049 (9)	Al(1)	N(20)	1.896 (9)
Ir(1)	C(30)	1.97 (1)	Al(1)	C(3)	1.97 (1)
Ir(2)	P(21)	2.284 (3)	Al(1)	C(4)	2.00 (1)
Ir(2)	P(22)	2.285 (3)	N(10)	C(10)	1.32 (1)
Ir(2)	C(20)	1.97 (1)	N(10)	C(11)	1.44 (1)
Ir(2)	C(40)	1.92 (1)	N(20)	C(20)	1.37 (1)
P(11)	C(1)	1.84 (1)	N(20)	C(21)	1.41 (1)
P(11)	C(111)	1.81 (1)	N(30)	C(30)	1.16 (1)
P(11)	C(112)	1.81 (1)	N(30)	C(31)	1.38 (1)
P(12)	C(2)	1.85 (1)	N(40)	C(40)	1.18 (1)
P(12)	C(121)	1.82 (1)	N(40)	C(41)	1.39 (1)
P(12)	C(122)	1.82 (1)	C(3)	C(5)	1.52 (2)
P(21)	C(1)	1.85 (1)	C(4)	C(6)	1.53 (2)
P(21)	C(211)	1.83 (1)	C(10)	C(20)	1.48 (1)
P(21)	C(212)	1.85 (1)	C(11)	C(12)	1.40 (2)
P(22)	C(2)	1.82 (1)	C(11)	C(16)	1.41 (2)
C(12)	C(13)	1.39 (2)	C(31)	C(36)	1.41 (2)
C(12)	C(17)	1.50 (2)	C(32)	C(33)	1.39 (2)
C(13)	C(14)	1.36 (2)	C(32)	C(37)	1.50 (2)
C(14)	C(15)	1.39 (2)	C(33)	C(34)	1.37 (2)
C(15)	C(16)	1.39 (2)	C(34)	C(35)	1.36 (2)
C(16)	C(18)	1.50 (2)	C(35)	C(36)	1.40 (2)
C(21)	C(22)	1.39 (2)	C(36)	C(38)	1.50 (2)
C(21)	C(26)	1.40 (2)	C(41)	C(42)	1.39 (1)
C(22)	C(23)	1.41 (2)	C(41)	C(46)	1.40 (2)
C(22)	C(27)	1.51 (2)	C(42)	C(43)	1.39 (2)
C(23)	C(24)	1.39 (2)	C(42)	C(47)	1.52 (2)
C(24)	C(25)	1.34 (2)	C(43)	C(44)	1.37 (2)
C(25)	C(26)	1.40 (2)	C(44)	C(45)	1.36 (2)
C(26)	C(28)	1.51 (2)	C(45)	C(46)	1.36 (2)
C(31)	C(32)	1.38 (1)	C(46)	C(48)	1.47 (2)

atom 1	atom 2	atom 3	angle[a]	atom 1	atom 2	atom 3	angle[a]
Ir(2)	Ir(1)	P(11)	84.43 (7)	C(20)	Ir(2)	C(40)	99.7 (4)
Ir(2)	Ir(1)	P(12)	94.87 (8)	Ir(1)	P(11)	C(1)	114.0 (4)
Ir(2)	Ir(1)	C(10)	68.6 (3)	Ir(1)	P(11)	C(111)	117.9 (4)
Ir(2)	Ir(1)	C(30)	170.4 (3)	Ir(1)	P(11)	C(112)	117.6 (5)
P(11)	Ir(1)	P(12)	101.5 (1)	C(1)	P(11)	C(111)	101.9 (6)
P(11)	Ir(1)	C(10)	92.3 (3)	C(1)	P(11)	C(112)	102.0 (6)
P(11)	Ir(1)	C(30)	99.1 (3)	C(111)	P(1)	C(112)	100.9 (6)
P(12)	Ir(1)	C(10)	157.5 (3)	Ir(1)	P(12)	C(2)	112.9 (4)
P(12)	Ir(1)	C(30)	93.2 (3)	Ir(1)	P(12)	C(121)	114.2 (4)
C(10)	Ir(1)	C(30)	102.2 (4)	Ir(1)	P(12)	C(122)	124.2 (5)
Ir(1)	Ir(2)	P(21)	94.74 (8)	C(2)	P(12)	C(121)	101.2 (7)
Ir(1)	Ir(2)	P(22)	85.91 (8)	C(2)	P(12)	C(122)	103.1 (7)
Ir(1)	Ir(2)	C(20)	73.2 (3)	C(121)	P(12)	C(122)	98.0 (7)
Ir(1)	Ir(2)	C(40)	170.4 (3)	Ir(2)	P(21)	C(1)	114.7 (4)
P(21)	Ir(2)	P(22)	100.3 (1)	Ir(2)	P(21)	C(211)	115.0 (5)
P(21)	Ir(2)	C(20)	121.6 (3)	Ir(2)	P(21)	C(212)	123.2 (5)
P(21)	Ir(2)	C(40)	94.5 (3)	C(1)	P(21)	C(211)	100.9 (7)
P(22)	Ir(2)	C(20)	133.9 (3)	C(1)	P(21)	C(212)	100.5 (6)
P(22)	Ir(2)	C(40)	95.0 (3)	C(211)	P(21)	C(212)	99.0 (8)
Ir(2)	P(22)	C(2)	116.6 (5)	C(40)	N(40)	C(41)	163 (1)
Ir(2)	P(22)	C(221)	115.5 (4)	P(11)	C(1)	P(21)	108.6 (6)
Ir(2)	P(22)	C(222)	120.2 (5)	P(12)	C(2)	P(22)	112.0 (6)
C(2)	P(22)	C(221)	102.4 (7)	Al(1)	C(3)	C(5)	113 (1)
C(2)	P(22)	C(222)	99.5 (6)	Al(1)	C(4)	C(6)	112.8 (9)
C(221)	P(22)	C(222)	99.5 (7)	Ir(1)	C(10)	N(10)	133.7 (7)
N10)	Al	N(20)	84.9 (4)	Ir(1)	C(10)	C(20)	110.3 (6)
N(10)	Al	C(3)	112.9 (5)	N(10)	C(10)	C(20)	115.8 (8)
N(10)	Al	C(4)	114.3 (5)	N(10)	C(11)	C(12)	119 (1)
N(20)	Al	C(3)	118.6 (5)	N(10)	C(11)	C(16)	120 (1)
N(20)	Al	C(4)	114.1 (5)	C(12)	C(11)	C(16)	121 (1)
C(3)	Al	C(4)	110.2 (5)	C(11)	C(12)	C(13)	119 (1)
Al	N(10)	C(10)	112.3 (7)	C(11)	C(12)	C(17)	121 (1)
Al	N(10)	C(11)	122.1 (7)	C(13)	C(12)	C(17)	119 (1)
C(10)	N(10)	C(11)	125.3 (8)	C(12)	C(13)	C(14)	121 (1)
Al	N(20)	C(20)	113.1 (7)	C(13)	C(14)	C(15)	120 (1)
Al	N(20)	C(21)	126.0 (7)	C(14)	C(15)	C(16)	122 (1)
C(20)	N(20)	C(21)	120.5 (8)	C(11)	C(16)	C(15)	117 (1)
C(30)	N(30)	C(31)	163 (1)	C(11)	C(16)	C(18)	121 (1)
C(15)	C(16)	C(18)	121 (1)	C(32)	C(31)	C(36)	122 (1)
Ir(2)	C(20)	N(20)	138.6 (8)	C(31)	C(32)	C(33)	118 (1)
Ir(2)	C(20)	C(10)	107.5 (6)	C(31)	C(32)	C(37)	121 (1)

Table IV (Continued)

atom 1	atom 2	atom 3	angle[a]	atom 1	atom 2	atom 3	angle[a]
N(20)	C(20)	C(10)	113.2 (8)	C(33)	C(32)	C(37)	120 (1)
N(20)	C(21)	C(22)	120 (1)	C(32)	C(33)	C(34)	120 (1)
N(20)	C(21)	C(26)	121 (1)	C(33)	C(34)	C(35)	121 (1)
C(22)	C(21)	C(26)	119 (1)	C(34)	C(35)	C(36)	122 (1)
C(21)	C(22)	C(23)	119 (1)	C(31)	C(36)	C(35)	116 (1)
C(21)	C(22)	C(27)	121 (1)	C(31)	C(36)	C(38)	122 (1)
C(23)	C(22)	C(27)	120 (1)	C(35)	C(36)	C(38)	122 (1)
C(22)	C(23)	C(24)	120 (1)	Ir(2)	C(40)	N(40)	170 (1)
C(23)	C(24)	C(25)	120 (1)	N(40)	C(41)	C(42)	119 (1)
C(24)	C(25)	C(26)	121 (1)	N(40)	C(41)	C(46)	120 (1)
C(21)	C(26)	C(25)	120 (1)	C(42)	C(41)	C(46)	122 (1)
C(21)	C(26)	C(28)	120 (1)	C(41)	C(42)	C(43)	118 (1)
C(25)	C(26)	C(28)	120 (1)	C(41)	C(42)	C(47)	121 (1)
Ir(1)	C(30)	N(30)	176.2 (9)	C(43)	C(42)	C(47)	120 (1)
N(30)	C(31)	C(32)	119 (1)	C(42)	C(43)	C(44)	120 (1)
N(30)	C(31)	C(36)	118 (1)	C(43)	C(44)	C(45)	120 (1)
C(44)	C(45)	C(46)	123 (1)	C(41)	C(46)	C(48)	121 (1)
C(41)	C(46)	C(45)	117 (1)	C(45)	C(46)	C(48)	122 (1)

[a] Numbers in parentheses are estimated standard deviations in the least significant digits.

N–Al–N angle of 80.9° compares well with the value of 84.0 (1) and 84.5 (1)° found in the structure of $(Ph_2C{=}N)_4Al_2(\mu\text{-}N{=}CPh_2)_2$.[46] The Ir–Ir bond length of 2.7861 (6) Å is well within the range of formal single bonds, but is considerably longer than that in **1** (2.5998 (7) Å). The Ir–C distances of 2.049 (10) and 1.970 (10) Å are slightly shorter than those in **1** (mean value of 2.073 Å).

EPR Studies of 3. Complex **3** has one unpaired electron, which is introduced by the formal addition of a neutral $^{\bullet}AlEt_2$ radical to the diamagnetic complex **1**. At −150 °C the EPR powder spectrum of **3** exhibits a broad isotropic signal with $g = 2.005$. The −150 °C powder EPR spectrum is presented in Figure 8. A total of 4500 hyperfine peaks are predicted for a system containing two Ir ($I = {}^3/_2$ for ^{191}Ir and ^{193}Ir), two N ($I = 1$), one Al ($I = {}^5/_2$), and four P ($I = {}^1/_2$) atoms. The rather broad, featureless spectrum is therefore attributed to unresolved hyperfine coupling. The completely isotropic nature of the low-temperature powder spectrum suggests that the unpaired electron of **3** resides in a molecular orbital with essentially no contribution from the iridium atoms, as indicated in eq 4. This result is in accord with IR ν(CN) data, which suggest that there is no change in the formal oxidation state of **3** compared to **1** and indicates the unpaired electron likely is delocalized exclusively within the C_2N_2Al ring of **3**.

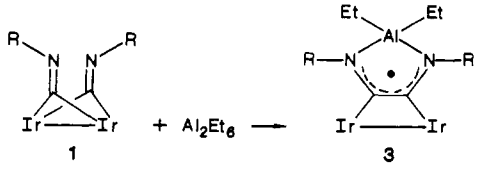

(4)

The Roles of Lewis Acids and Electron Transfer in Carbon–Carbon Bond Formation. The formation of a new carbon–carbon bond in **3** by annulation of two μ-isocyanides with an $^{\bullet}AlEt_2$ radical is unprecedented.[47] The structure of the product **3** provides few clues concerning the mechanism of formation of the new carbon–carbon bond. The coupling of isocyanides in the transformation **1** + Al_2Et_6 → **3** differs significantly from other reported carbonyl or isocyanide coupling reactions,[5,7,9] since it does not appear to require two electrons from an external reducing agent. Moreover, the structure and IR and EPR spectroscopic data for **3** imply that the electrons required for C–C bond formation apparently are not derived from the diiridium(0) core. A careful examination of the reaction of **1** with Al_2Et_6, however, suggests that an internal electronic reconfiguration of the diiridium framework from a d^9–d^9 cradle to a d^8–d^8 A-frame drives the isocyanide coupling reaction. In the initial phase of the reaction

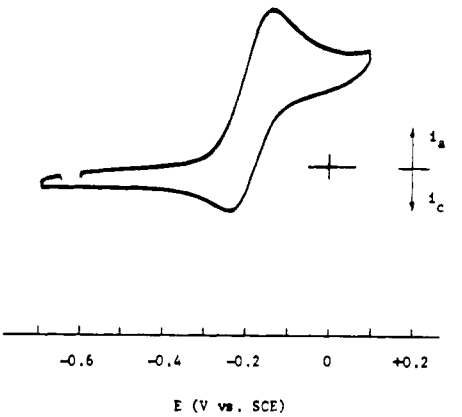

Figure 9. Cyclic voltammogram of $Ir_2\{C_2(NR)_2AlEt_2\}(CNR)_2(dmpm)_2$ **3** in THF solution. Supporting electrolyte: 0.1 M tetra-*n*-butylammonium tetrafluoroborate. Reference electrode: saturated calomel electrode (SCE).

of **1** with Al_2Et_6, the complexation of 1 equiv of $AlEt_3$ with **1** is observed by NMR (vide supra), eq 5. The $^{\bullet}AlEt_2$ radical found

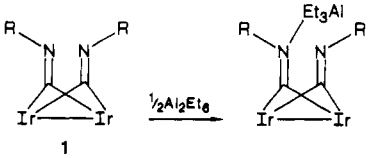

(5)

in **3** appears to be formed by displacement of $C_2H_5^-$ and abstraction by the second equivalent of $AlEt_3$ to give $AlEt_4^-$, eq 6.

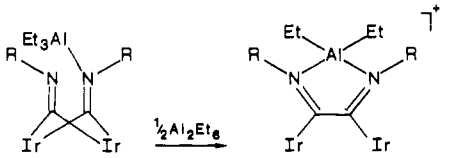

(6)

Schmidbaur has reported an apparently similar annulation with Al_2Me_6 in the case of bis(trialkylphosphoranylimino)silanes,[48] eq 7. Upon abstraction of $C_2H_5^-$ from the initial adduct, one would

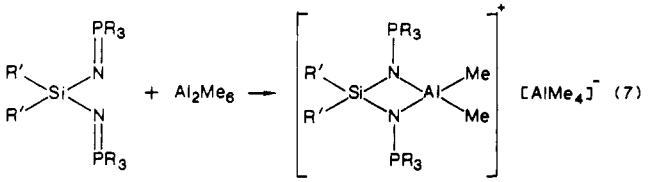

(7)

(46) Bryan, S. J.; Clegg, W.; Snaith, R.; Wade, K.; Wong, E. H. *J. Chem. Soc., Chem. Commun.* **1987**, 1223.

(47) A similar annulation involving $C_6H_5CH{=}NC_6H_5$, $R_3Al{\cdot}THF$, and potassium has been described: Lehmkuhl, H. *Chimia* **1970**, *24*, 182.

(48) Schmidbaur, H.; Wolfsberger, W.; Schwirten, K. *Chem. Ber.* **1969**, *102*, 556.

expect formation of the species $[Ir_2\{C_2(NR)_2AlEt_2\}(CNR)_2(dmpm)_2]^+[AlEt_4]^-$, **4**·$[AlEt_4^-]$. Indeed the molecular cation **4** can be prepared chemically and electrochemically by one-electron oxidation of **3**.[49] Cyclic voltammetric studies of **3** in THF solution reveal one reversible oxidation at −0.22 V (ΔE_{p-p} = 90 mV) vs SCE, Figure 9. In coulometric studies, a one-electron oxidation of **3** in THF at +0.3V vs SCE is accompanied by a dramatic color change from red-purple to yellow. The same phenomenon is observed when **3** is oxidized chemically by 1 equiv of $[Cp_2Fe][PF_6]$ in THF solution. Both chemical and electrochemical oxidation give the same diamagnetic product, **4**, which exhibits a signal at

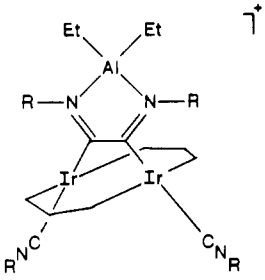

4

δ −43.3 ppm in its $^{31}P\{^1H\}$ NMR spectrum. The $^{31}P\{^1H\}$ NMR spectrum of paramagnetic **3** was not observable. The ^{31}P NMR chemical shift of **4** at δ −43.3 ppm is similar to that of $[Ir_2(CNR)_5(dmpm)_2][PF_6]_2$ (δ −44.1 ppm for dmpm).[14] The FTIR spectrum of **[4]**$[PF_6]$ in KBr exhibits a terminal isocyanide ν(CN) band at 2123 cm^{-1}, more than 80 cm^{-1} higher than those of **1** and **3**, but very similar to the Ir(I) complexes $[Ir_2(CNR)_5(dmpm)_2][PF_6]_2$ (2121 and 2101 cm^{-1}) and $[Ir_2(\mu\text{-}H)_2(CNR)_4(dmpm)_2][PF_6]_2$ (R = 2,6-$Me_2C_6H_3$) (2146 and 2127 cm^{-1}).[14] In the bridging ν(CN) region between 1700 and 1450 cm^{-1}, however, no band can be assigned to C=N double bonds. This implies that the carbon–carbon bond in the C_2N_2Al ring of **3** does not cleave in the oxidation process to **4**. In the ν(PC) region, only one sharp band is observed at 943 cm^{-1}. This band is superimposable on the ν(PC) of structurally characterized *trans,trans*-$M_2(dmpm)_2$ complexes, such as **4** $[Ir_2(CNR)_5(dmpm)_2][PF_6]_2$. Therefore, an A-frame structure is assigned to **4**. In **4**, each Ir atom has a formal +1 oxidation state. This is consistent with the terminal ν(CN) bands at 2123 cm^{-1} and $^{31}P\{^1H\}$ NMR chemical shift of δ −43.3 ppm. The FTIR and $^{31}P\{^1H\}$ studies therefore suggest that one-electron oxidation of **3** to **4** induces an isomerization from a cradle to an A-frame structure.

The overall coupling scheme is depicted in Scheme I and can be summarized as follows: (i) complexation of one $AlEt_3$ with **1**; (ii) annulation of $AlEt_2^+$ and coupling of the two μ-isocyanide ligands to produce **4**, with transfer of Et^- to a second equivalent of $AlEt_3$; (iii) Under the reaction conditions, **4** is reducible in an electron-transfer sense to give the isolated radical species, **3**. We note the direct reaction of **4** with $AlEt_4^-$ produces **3**. The resulting $AlEt_3$ radical apparently decomposes with loss of C_2H_4 and C_2H_6, both of which are detected by GC during the reaction.

Attempted Coupling Reactions of 1 with Other Reagents. Our results suggest that the carbon–carbon bond of **3** is produced by intramolecular electron transfer from the Ir^0_2 core of **1** to its μ-isocyanide ligands. The overall reductive coupling of the isocyanide ligands is induced by the reaction with a Lewis acid, $AlEt_3$. The presumed intermediate **4** differs from **1** by the presence of an $AlEt_2^+$ fragment. We have examined the coupling of the μ-isocyanides of **1** by the addition of other electron-deficient reagents. For example the reagents AlR_2Cl were expected to eliminate Cl^- faster than $AlEt_3$ eliminates "Et^-" in the formation of **4**. The reaction of **1** with $AlMe_2Cl$, however, produced unstable iridium chloride complexes, which were not isolable.

The reaction of **1** with BF_3·OEt_2 gives a pale yellow compound. This compound exhibits bridging ν(CN) at 1507 cm^{-1}, representing a significant decrease compared to **1**, similar to the reaction of **1** with BH_3·THF leading to **2**. In contrast to **2**, this yellow product exhibits a sharp ν(PC) band at 943 cm^{-1}, suggesting an A-frame structure. The complex also exhibits ν(B–F) = 1087 (s), 1060 (vs), 1037 (s) cm^{-1}. The very strong band at 1060 cm^{-1} corresponds to BF_4^-. A product that can accommodate an A-frame structure is a carbon–carbon coupled product. It is suggested that the reaction of **1** with BF_3·THF induces isocyanide coupling, leading to an A-frame product, $[Ir_2(\eta^2\text{-}(CNR)_2BF_2)(CNR)_2(dmpm)_2][BF_4^-]$, with a structure similar to **4**.

Scheme I

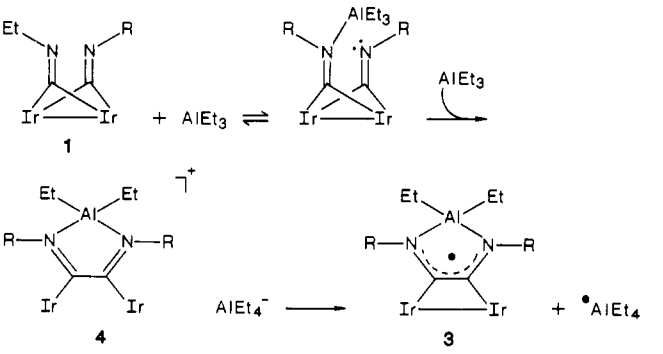

Similarly, the reaction of **1** with maleic anhydride leads to a red solid. This product also exhibits a sharp ν(PC) band at 941 cm^{-1} and a $^{31}P\{^1H\}$ NMR chemical shift at δ −43.9 ppm (CH_2Cl_2), very close to that of **4**, and consistent with a carbon–carbon coupled A-frame structure. The reaction of **1** with maleic anhydride may represent [2 + 2 + 2] cycloaddition of an electron-deficient olefin with a pair of bridging isocyanide ligands. The cycloaddition chemistry of **1** is a subject of continuing investigation.

Conclusion. The binuclear iridium(0) complex **1** has been prepared from Na/Hg reduction of a mixture of $[IrCl(COD)]_2$, 2,6-xylyl isocyanide, and dmpm. Complex **1** possesses a cradle-type structure and a very short nonbonded C···C contact of 2.37 (2) Å for the μ-isocyanide ligands. The nitrogen atoms of the μ-CNR ligands are basic in the Lewis sense and react with Lewis acids efficiently. Carbon–carbon bond forming reactions between the μ-isocyanide ligands of **1**, induced by Lewis acids, were investigated. Reaction of **1** with BH_3·THF results in a bis(μ-aminocarbyne) complex, **2**, which has a cradle structure similar to **1**. This reaction does not induce carbon–carbon coupling.

Reaction of **1** with Al_2Et_6 induces a carbon–carbon bond coupling between the μ-isocyanide ligands, leading to **3**. The newly formed carbon–carbon bond is parallel to the Ir–Ir bond and can be described as 1,2-dimetalated olefin. Complex **3** has an unpaired electron and exhibits an isotropic EPR spectrum at −150 °C with g = 2.005. The unpaired electron is apparently delocalized exclusively within the C_2N_2Al ring of **3**. Complex **3** exhibits a reversible one-electron oxidation at −0.22 V vs SCE. Both chemical and electrochemical oxidation of **3** lead to a cation **4**. This oxidation is accompanied by an isomerization from cradle (**3**) to A-frame (**4**) structure. Reactions of **1** with BF_3·OEt_2 and maleic anhydride lead to carbon–carbon coupling products apparently similar to the A-frame structure of **4**. This type of carbon–carbon bond forming reaction differs from other coupling reactions of coordinated ligands in that it does not require two electrons from an external reducing agent. The two reducing electronic equivalents come from d^9–d^9 cradle → d^8–d^8 A-frame electronic reconfiguration. This work is directly relevant to the mechanisms of carbon–carbon bond formation between C_1 substrates and suggests a potentially important cocatalytic role of Lewis acids.

Acknowledgment. This work was supported by the National Science Foundation (Grant CHE-8707963). NSF support of the Chemical X-ray Diffraction Facility is also gratefully acknowledged. A generous loan of iridium trichloride from Johnson-Matthey, Inc. is also gratefully acknowledged.

(49) A similar case of using multiply bonded ditungsten complexes to promote carbon–carbon bond formation through reduction coupling of ketones has been reported; see: Anderson, L. B.; Cotton, F. A.; DeMarco, D.; Falvello, L. R.; Tetrick, S. M.; Walton, R. A. *J. Am. Chem. Soc.* **1984**, *106*, 4743.

Supplementary Material Available: Tables of atomic positions and their estimated standard deviations and calculated hydrogen atom positions for **1–3** (Tables 1, 5, and 8), general temperature factor expressions for **1–3** (Tables 2, 6, 9), and least-squares planes and dihedral angles for **1** and **3** (Tables 3 and 10) (25 pages); observed and calculated structure factors for **1–3** (Tables 4, 7, and 11) (63 pages). Ordering information is given on any current masthead page.

Cleavage of SO_2 on $(\eta^5\text{-}C_5Me_5)_2Mo_2(\mu\text{-}S_2)(\mu\text{-}S)_2$ To Form S_8 and a Thiosulfate Complex, $(\eta^5\text{-}C_5Me_5)_2Mo_2(\mu\text{-}S_2)(\mu\text{-}S)(\mu\text{-}SSO_3)$. Possible Role in Homogeneous Hydrogenation of SO_2 Catalyzed by Mo–S Complexes

Gregory J. Kubas,* Robert R. Ryan, and Kimberly A. Kubat-Martin

Contribution from the Inorganic and Structural Group (INC-4), Los Alamos National Laboratory, MS C346, Los Alamos, New Mexico 87545. *Received March 8, 1989*

Abstract: Reaction of SO_2 with solutions of $Cp^*_2Mo_2(\mu\text{-}S_2)(\mu\text{-}S)_2$ (**1**) initially yields **1**·SO_2, which is shown by crystallography to contain an SO_2 weakly bound to a μ-S (S–S = 2.60 Å). SO_2 further reacts with **1**·SO_2 to quantitatively give $Cp^*_2Mo_2(\mu\text{-}S_2)(\mu\text{-}S)(\mu\text{-}SSO_3)$ (**2**), which now contains an SO_3 bound to the μ-S (S–S = 2.17 Å). Effectively, a μ-S_2O_3 (thiosulfate) ligand is formed by an oxygen-transfer process, and *the source of the oxygen as established by* ^{18}O *labeling is* SO_2. S_8 is also produced, showing that SO_2 has undergone net disproportionation to SO_3 and S_8. The reaction rate is highly dependent on solvent polarity and base promoters such as Et_3N. Sterically hindered amines do not accelerate the reaction, suggesting that they function as Lewis rather than Brønsted bases. The X-ray structure of **2** is identical with that of a complex formed in low yield (along with dimeric oxosulfido complexes) by air oxidation of **1**. **2** is readily hydrogenated at 25–75 °C to regenerate **1**, indicating that the mechanism of the previously studied hydrogenation of SO_2 to S_8 and H_2O catalyzed by Mo–S complexes may involve **2** as an intermediate. Weak bases, e.g., Et_3N, strip off the SO_3 functionality in **2** to give primarily mixtures of isomers of **1** and products of base–SO_3 interaction. Crystallographic data for $Cp^*_2Mo_2(\mu\text{-}S_2)(\mu\text{-}S)(\mu\text{-}S\text{·}SO_2)$: space group $P2_1/c$; a = 13.738 (2) Å, b = 10.581 (3) Å, c = 17.331 (4) Å, β = 92.41 (2)°; V = 2516.9 Å^3 at 296 K; D_{calc} = 1.73 g/cm^{-1} for Z = 4; R = 6.2% for 2017 independent reflections with $I \geq 2\sigma(I)$ and $2\theta \leq 45°$. Crystallographic data for $Cp^*_2Mo_2(\mu\text{-}S_2)(\mu\text{-}S)(\mu\text{-}SSO_3)$: space group $P2_1/c$; a = 13.730 (5) Å, b = 10.635 (3) Å, c = 16.862 (2) Å, β = 93.17 (5)°; V = 2458.5 Å^3 at 296 K; D_{calc} = 1.81 g/cm^{-1} for Z = 4; R = 4.0% for 2612 reflections with $I \geq 2\sigma(I)$ and $2\theta \leq 45°$.

The activation of S=O bonds in SO_2 by transition-metal complexes, particularly toward reduction by hydrides and hydrogen,[1-6] has been a major recent focus of our research. We have shown[1] that the complexes investigated by Rakowski DuBois and co-workers,[7] $[(Me_nCp)Mo(\mu\text{-}S)(\mu\text{-}SH)]_2$, where n = 0, 1, or 5 (Cp*), catalyze homogeneous hydrogenation of SO_2 to S_8 and H_2O (eq 1) and react stoichiometrically with SO_2 as in eq 2:

$$SO_2 + 2H_2\ (2\text{–}3\ \text{atm}) \xrightarrow[350\ \text{turnovers/h}]{\text{PhCl–BuOH, 75°C}} \tfrac{1}{8}S_8 + 2H_2O \quad (1)$$

The disulfide-bridged product, $Cp^*_2Mo_2(\mu\text{-}S_2)(\mu\text{-}S)_2$ (**1**), had previously been prepared and structurally characterized by Wachter's group,[8] and polymeric, insoluble $(Cp^*MoS_x)_n$ (x = ~3)[9] is the synthetic precursor to $[Cp^*MoS(SH)]_2$.[7] Both Mo

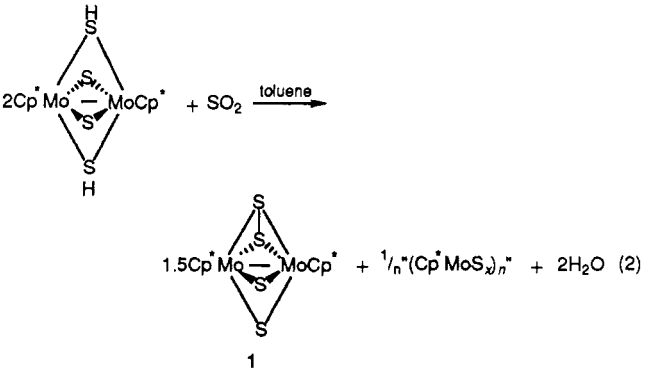

products of eq 2 react with H_2 under mild conditions similar to those in the catalytic reaction (eq 1) to regenerate the SH complex.[1,7,8b] Thus, eq 2 was believed to be a logical first step in the mechanism for catalytic reduction of SO_2.[1] In order to gain more information on the role of **1** in the catalysis, we have studied the reactivity of **1** (and to a partial extent its MeCp analogue) with SO_2 and other oxygen-containing small molecules (SO_3, O_2) and report the results here.[10]

The formation of an SO_2 adduct of **1**, $Cp^*_2Mo_2(\mu\text{-}S_2)(\mu\text{-}S)(\mu\text{-}S\text{·}SO_2)$, **1**·$SO_2$, with the SO_2 bound to a μ-S ligand, was not

(1) Kubas, G. J.; Ryan, R. R. *J. Am. Chem. Soc.* **1985**, *107*, 6138.
(2) Kubas, G. J.; Ryan, R. R. *Inorg. Chem.* **1984**, *23*, 3181.
(3) Kubas, G. J.; Wasserman, H. J.; Ryan, R. R. *Organometallics* **1985**, *4*, 2012.
(4) Kubas, G. J.; Wasserman, H. J.; Ryan, R. R. *Organometallics* **1985**, *4*, 419.
(5) Kubas, G. J.; Ryan, R. R. *Polyhedron* **1986**, *5*, 473.
(6) (a) Kubat-Martin, K. A.; Kubas, G. J.; Ryan, R. R. *Organometallics*, **1988**, *7*, 1657. (b) Kubat-Martin, K. A.; Kubas, G. J.; Ryan, R. R. *Organometallics*, in press.
(7) (a) Rakowski DuBois, M.; VanDerveer, M. C.; DuBois, D. L.; Haltiwanger, R. C.; Miller, W. K. *J. Am. Chem. Soc.* **1980**, *102*, 7456. (b) Casewit, C. J.; Coons, D. E.; Wright, L. L.; Miller, W. K.; Rakowski DuBois, M. *Organometallics*, **1986**, *5*, 951.
(8) (a) Brunner, H.; Meier, W.; Wachter, J.; Guggolz, E.; Zahn, T.; Ziegler, M. L. *Organometallics*, **1982**, *1*, 1107. (b) Brunner, H.; Kauermann, H.; Meier, W.; Wachter, J. *J. Organomet. Chem.* **1984**, *263*, 183.
(9) (a) Schunn, R. A.; Fritchie, C. J., Jr.; Prewitt, C. T. *Inorg. Chem.* **1966**, *5*, 892. (b) Rakowski DuBois, M.; DuBois, D. L.; VanDerveer, M. C.; Haltiwanger, R. C. *Inorg. Chem.* **1981**, *20*, 3064.

(10) A portion of this work has been previously presented: Kubas, G. J.; Ryan, R. R.; Kubat-Martin, K. A. *Abstracts of Papers*, 194th National Meeting of the American Chemical Society, New Orleans, LA; American Chemical Society: Washington, DC, 1987; Paper INOR 256. Both we and Wachter's group (ref 11) independently synthesized and structurally characterized **2**.

0002-7863/89/1511-7823$01.50/0